CHAPTER 3
RESULTS AND DISCUSSION

3.1 Preparation and resolution of optically active monoacid–anthracene adducts (+)-(11*S*)-102 and (–)-(11*R*)-102 as starting material

Synthesis of enantiomerically pure *N*,*O* heteroatoms TADDOLs–like anthracene adducts as asymmetric ligands were stated by Diels–Alder reaction between anthracene and dimethyl itaconate and then resolution of the racemic dimethyl itaconate–anthracene adduct ((±)-**100**). These method were reported by Kongsaeree *et al*. in 2001[31], the racemic adduct (±)-**100** was resoluted by hydrolysis with NaOH (1.3 equiv) in solution of MeOH:H_2O (2:1) for 2 h. to give racemic monoacid–anthracene adduct (±)-**102** in 50% yield.

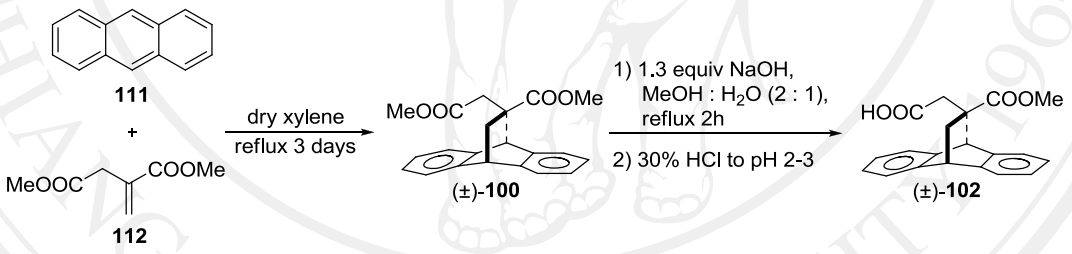

Scheme 19 Preparation of racemic monoacid–anthracene adduct (±)-**102**.

After that, the racemic adduct (±)-**102** was converted to diastereomeric compounds by treating with DMAP (0.2 equiv), DCC (1.2 equiv) and (–)-menthol (1.2 equiv) as a chiral auxiliary in dry CH_2Cl_2 at 0 °C to room temperature for overnight. The crude product was purified by crystallization to obtain two diastereoisomers of monomenthyl–anthracene adducts, (–)-(11*S*)-**101a** (43% yield), $[\alpha]_{589}^{28.0}$ = –14.21° (*c* = 0.219, $CHCl_3$) and (–)-(11*R*)-**101b** (43% yield), $[\alpha]_{589}^{28.7}$ = –61.35° (*c* = 0.163, $CHCl_3$).

Both of optically active pure dimethyl itaconate–anthracene adducts ((+)-(11*S*)-**100** and (–)-(11*R*)-**100**) were obtained by transmethylation of the two monomenthyl–

anthracene, (–)-(11*S*)-**101a** and (–)-(11*R*)-**101b** in excess anhydrous MeOH with sulfuric acid as catalyst, respectively. The products were purified by crystallization in CH_2Cl_2/hexane to give the both of optically active pure dimethyl itaconate–anthracene adducts, (+)-(11*S*)-**100** (87% yield), $[\alpha]_{589}^{24.8}$ = +38.74° (*c* = 0.327, $CHCl_3$) and (–)-(11*R*)-**100** (80% yield), $[\alpha]_{589}^{24.9}$ = –37.62° (*c* = 0.443, $CHCl_3$).

Then the both of optically active pure dimethyl itaconate–anthracene adducts ((+)-(11*S*)-**100** and (–)-(11*R*)-**100**) were hydrolyzed with NaOH (1.3 equiv) in solution of MeOH:H_2O (2:1) for 2 hours, followed by crystallization in CH_2Cl_2/hexane to give optically active pure monoacid–anthracene adducts, (+)-(11*S*)-**102** (96% yield), $[\alpha]_{589}^{27.6}$ = +45.45° (*c* = 0.176, $CHCl_3$) and (–)-(11*R*)-**102** (98% yield), $[\alpha]_{589}^{24.9}$ = –40.45° (*c* = 0.356, $CHCl_3$).

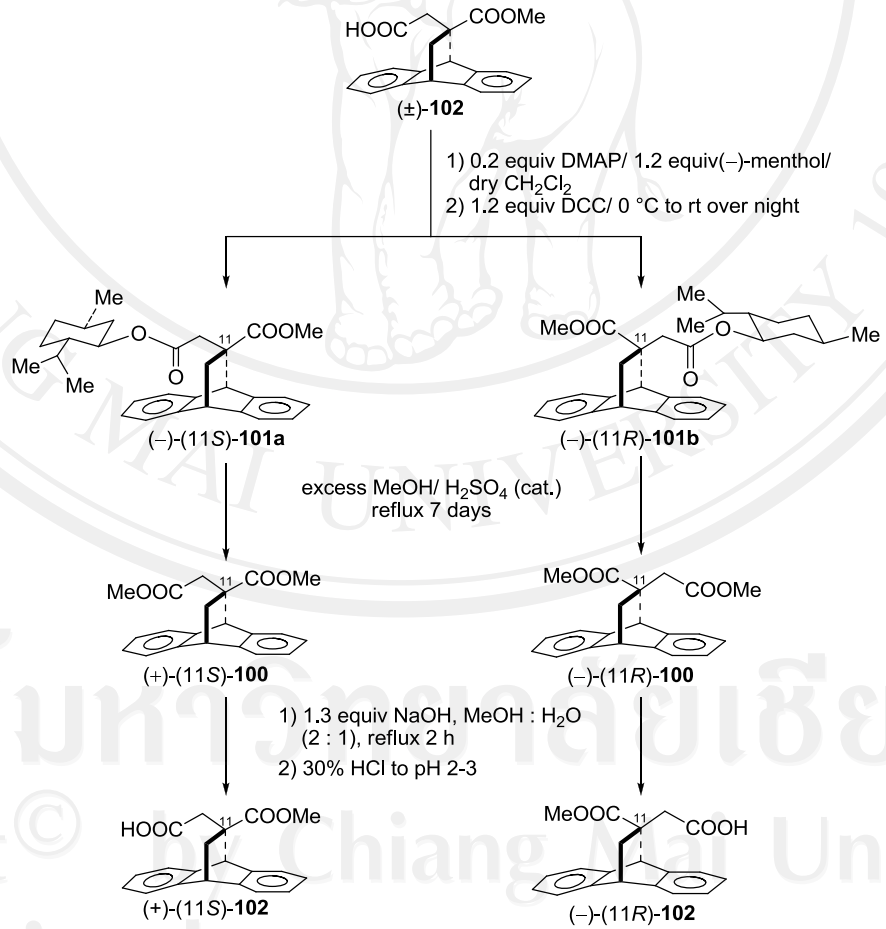

Scheme 20 Resolution of optically active monoacid–anthracene adducts (+)-(11*S*)-**102** and (–)-(11*R*)-**102**.

3.2 Synthesis of optically active amide–anthracene adducts (+)-(11*S*)-103, (–)-(11*R*)-103, (+)-(11*S*)-104 and (–)-(11*R*)-104

3.2.1 Synthesis of both optically active pure 11-carbomethoxy-11-pyrrolidinylacetyl-9,10-dyhydro-9,10-ethanoanthracene ((+)-(11*S*)-103 and (–)-(11*R*)-103)

The both enantiomeric pure pyrrolidinyl amide–anthracene adducts (+)-(11*S*)-**103** and (–)-(11*R*)-**103** were prepared from monoacid–anthracene adducts (+)-(11*S*)-**102** and (–)-(11*R*)-**102**, respectively. The monoacid–anthracene adducts were converted to acid chloride–anthracene adducts (+)-(11*S*)-**113** and (–)-(11*R*)-**113** by oxalyl chloride (1.5 equiv) in dry CH_2Cl_2 at room temperature and stirred for 1hour. After that, the mixtures were treated with pyrrolidine (2.0 equiv) and Et_3N (1.3 equiv) at 0 °C and stirred at room temperature for overnight. The products were purified by flash column chromatography (Acetone/EtOAc/hexane = 1:2:7 as eluent) to provide the both enantiomeric pure pyrrolidinyl amide–anthracene adducts, (+)-(11*S*)-**103** (93% yield), $[\alpha]_{589}^{29.6}$ = +54.47° (*c* = 0.235, $CHCl_3$) and (–)-(11*R*)-**103** (79% yield), $[\alpha]_{589}^{28.6}$ = –57.03° (*c* = 0.263, $CHCl_3$) (Scheme 21).

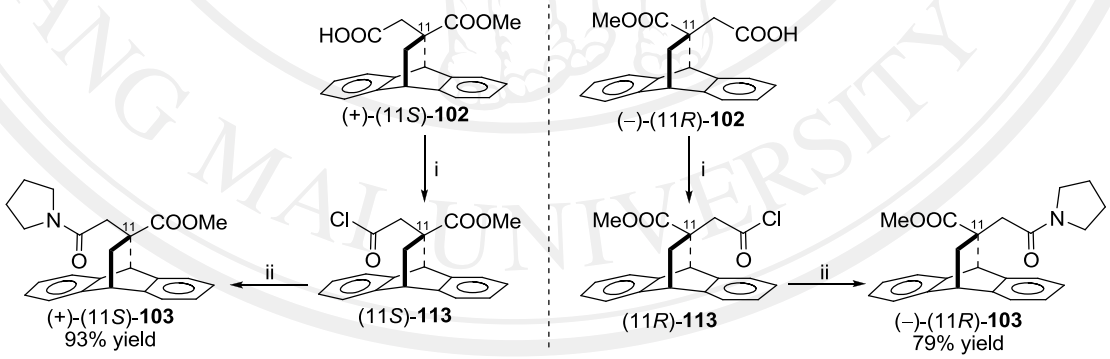

Scheme 21 Synthesis of both enantiomeric pure pyrrolidinyl amide–anthracene adducts (+)-(11*S*)-**103** and (–)-(11*R*)-**103**. *Reagents and conditions*: (i) 1.5 equiv $(COCl)_2$, dry CH_2Cl_2, N_2, rt, 1h; (ii) 2.0 equiv pyrrolidine, 1.3 equiv Et_3N, dry CH_2Cl_2, N_2, 0 °C to rt, overnight.

The structure of adducts (+)-(11*S*)-**103** and (–)-(11*R*)-**103** can be determined on the basis of spectroscopic data. In particular, the ^{1}H-NMR spectrum of these

adducts are shown in Figure 5. Proton H_a, H_b and H_x showed the signal at 1.44, 2.88 and 4.30 ppm (*ABX* system, (*J* = 13.2, 3.1 and 2.4 Hz), proton H_c and H_d at 1.90 ppm as doublet (*J* = 16.3 Hz) and 2.29 ppm as doublet (*J* = 16.3 Hz), proton H_y at 4.32 ppm as singlet and aromatic protons at 7.00-7.33 ppm as multiplet. In addition, the signal of protons on pyrrolidine ring, which are two protons on methylene C-2′and methylene C-3′ appeared at 1.68-1.86 ppm as multiplet, two protons on methylene C-1′ appeared at 2.29 ppm as doublet of doublet (*J* = 10.2 and 6.7 Hz) and 3.18 ppm as doublet of doublet (*J* = 10.2 and 6.7 ppm) and two protons of methylene C-4′ appeared at 3.41–3.26 ppm as multiplet. The correlation protons on H_a, H_b, H_c, H_d and protons on pyrrolidine ring were confirmed by COSY correlation. Furthermore, HMQC correlation showed that H_c and H_d correlated with methylene C-13 and proton on pyrrolidine ring correlated with C-1′, C-2′, C-3′ and C-4′. HMBC correlation indicated the connectivity between H_c and H_d with quaternary C-11 and C-14.

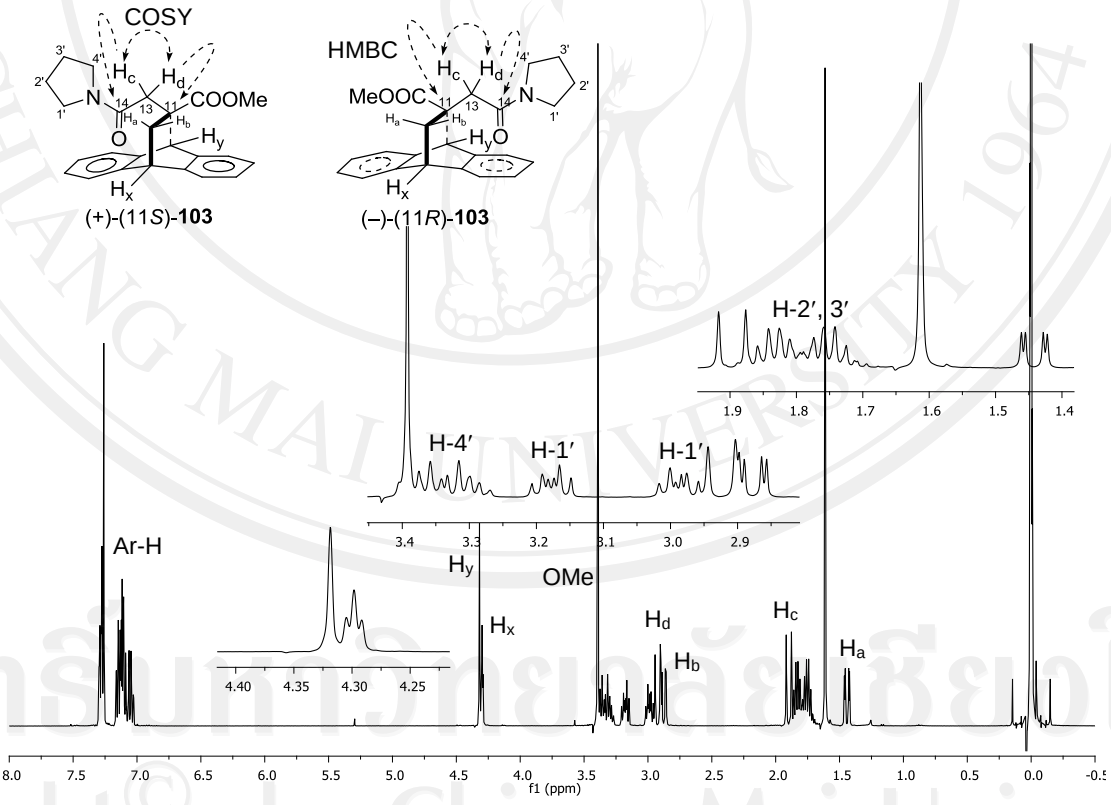

Figure 5 ^{1}H-NMR spectral data of pyrrolidinyl amide–anthracene adducts (+)-(11*S*)-**103** and (–)-(11*R*)-**103** (Dash arrows and plain arrows were COSY and HMBC correlation)

3.2.2 Synthesis of both optically active pure 11-carbomethoxy-11-piperidinylacetyl-9,10-dyhydro-9,10-ethanoanthracenes [(+)-(11*S*)-104 and (–)-(11*R*)-104]

The both enantiomeric pure piperidinyl amide–anthracene adducts (+)-(11*S*)-**104** and (–)-(11*R*)-**104**, which were prepared according to synthesis of pyrrolidinyl amide–anthracene adducts (Sec. 3.2.1) are shown in Scheme 22. The monoacid–anthracene adducts were converted to acid chloride–anthracene adducts followed by treatment with piperidine (2.0 equiv) and Et_3N (1.3 equiv) at 0 °C and stirred at room temperature for overnight. The products were purified by flash column chromatography (EtOAc/hexane = 4:6 as eluent) to obtain the both enantiomeric pure piperidinyl amide–anthracene adducts, (+)-(11*S*)-**104** (90% yield), $[\alpha]_{589}^{29.1}$ = +55.56° (*c* = 0.279, $CHCl_3$) and (–)-(11*R*)-**104** (82% yield), $[\alpha]_{589}^{28.7}$ = –55.56° (*c* = 0.225, $CHCl_3$).

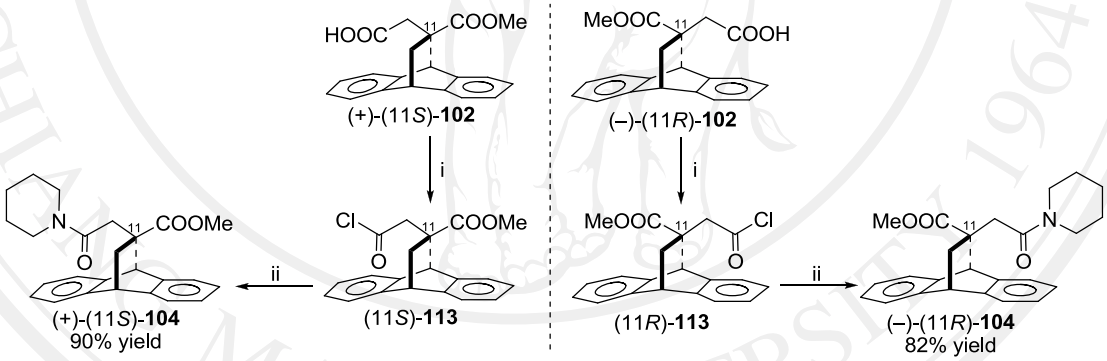

Scheme 22 Synthesis of both enantiomeric pure piperidinyl amide–anthracene adducts (+)-(11*S*)-**104** and (–)-(11*R*)-**104**. *Reagents and conditions*: (i) 1.5 equiv $(COCl)_2$, dry CH_2Cl_2, N_2, rt, 1h; (ii) 2.0 equiv piperidine, 1.3 equiv Et_3N, dry CH_2Cl_2, N_2, 0 °C to rt, overnight.

The structure of adducts (+)-(11*S*)-**104** and (–)-(11*R*)-**104** can be confirmed by NMR techniques. The ^{1}H-NMR spectrum of these adducts are illustrated in Figure 6. The signal of proton H_a, H_b and H_x appeared at 1.41, 2.87 and 4.29 ppm (*ABX* system, (*J* = 13.3, 3.0 and 2.5 Hz), proton H_c and H_d at 1.94 ppm as doublet (*J* = 16.2 Hz) and 2.98 ppm as doublet (*J* = 16.2 Hz), proton H_y at 4.29 ppm as singlet and aromatic protons at 6.96–7.36 ppm as multiplet. In addition, the signal of protons on

piperidine ring, which are six protons on methylene C-2′, methylene C-3′ and methylene C-4′ appeared at 1.32–1.70 ppm as multiplet, two protons on methylene C-1′ appeared at 3.01–3.07 and 3.08–3.21 ppm as multiplet and two protons of methylene C-5′ appeared at 3.23–3.36 and 3.45–3.58 ppm as multiplet. The correlation protons on H_a, H_b, H_c, H_d and protons on pyrrolidine ring were confirmed by COSY correlation. Besides, HMQC correlation showed that H_c and H_d correlated with methylene C-13 and proton on pyrrolidine ring correlated correlated with C-1′, C-2′, C-3′, C-4′ and C-5′. HMBC correlation showed that proton H_c and H_d correlated with quaternary C-11 and C-14.

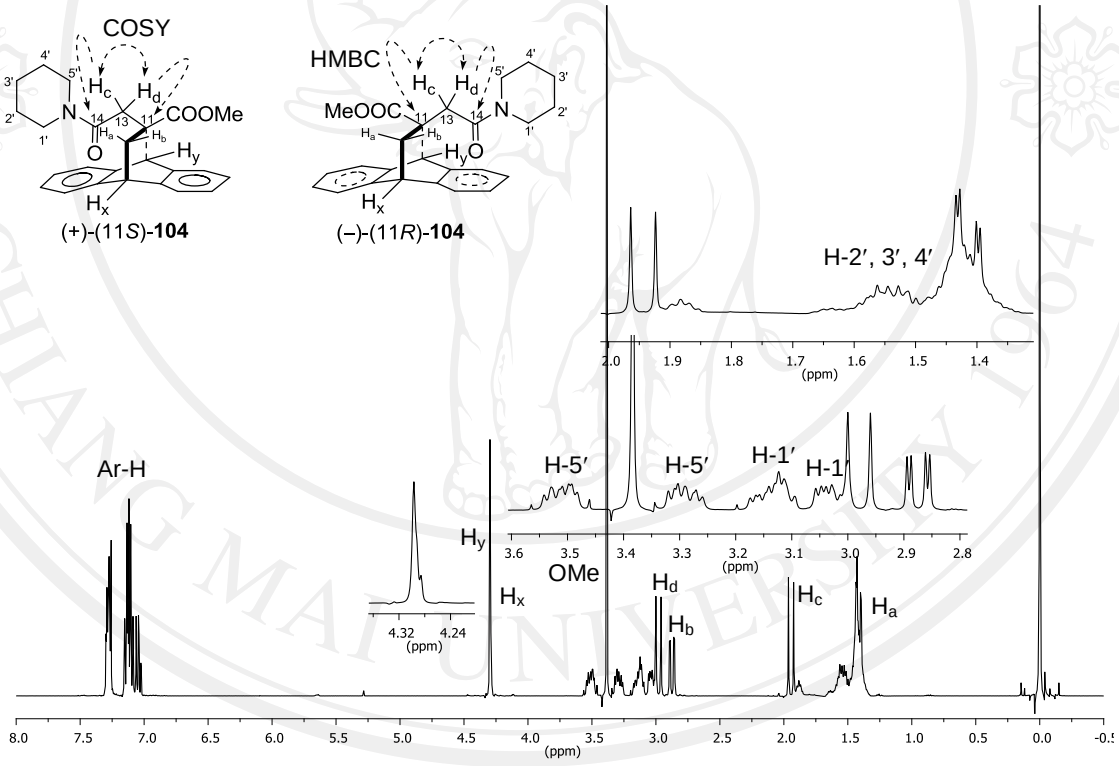

Figure 6 ^{1}H-NMR spectral data of piperidinyl amide–anthracene adducts (+)-(11*S*)-**104** and (–)-(11*R*)-**104** (Dash arrows and plain arrows were COSY and HMBC correlation)

3.3 Derivatization of optically active amide–anthracene adducts (+)-(11*S*)-103, (–)-(11*R*)-103, (+)-(11*S*)-104 and (–)-(11*R*)-104

3.3.1 Synthesis of diastereomeric benzyl(piperidinyl or pyrrolidinyl) amide–anthracene adducts ((11*S*)-114, (11*R*)-114, 11(*S*)-116 and (11*R*)-116)

Substitution reaction with benzyl bromide of amide–anthracene adducts (+)-(11*S*)-**103**, (–)-(11*R*)-**103**, (+)-(11*S*)-**104** and (–)-(11*R*)-**104** were studied by varying the stoichiometric equivalent of lithium diisopropylamide (LDA). Firstly, substitution reaction with benzyl group of adducts (+)-(11*S*)-**103** and (+)-(11*S*)-**103** were used as model reaction (Table 25).

Table 25 Optimization of synthetic benzylamide–anthracene adducts (11*S*)-**114** and (11*S*)-**116**

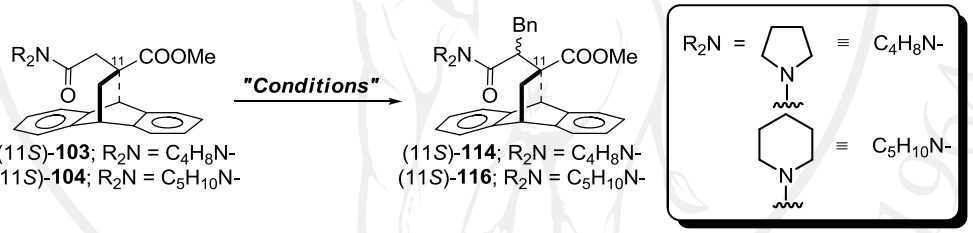

Entry	R_2N	Conditions	Yield (%)[a]	Conversion (%)
1	C_4H_8N-	i) 1.2 equiv LDA, THF, –78 °C to 0 °C, N_2, 2 h ii) 2.0 equiv BnBr, –78 °C to rt, N_2, overnight	93	53
2		i) 2.5 equiv LDA, THF, –78 °C to 0 °C, N_2, 2 h ii) 2.0 equiv BnBr, –78 °C to rt, N_2, overnight	57	93
3	$C_5H_{10}N$-	i) 1.2 equiv LDA, THF, –78 °C to 0 °C, N_2, 2 h ii) 2.0 equiv BnBr, –78 °C to rt, N_2, overnight	98	79
4		i) 2.5 equiv LDA, THF, –78 °C to 0 °C, N_2, 2 h ii) 2.0 equiv BnBr, –78 °C to rt, N_2, overnight	Complex mixtures	

[a] Isolated yield

From Table 25, entry 1-4 illustrated the substitution reaction of amide–anthracene adducts with benzyl bromide. We found that pyrrolidinyl amide–anthracene adduct (+)-(11*S*)-**103** and piperidinyl amide–anthracene adduct (+)-(11*S*)-

103 were reacted with 1.2 equivalents of lithium diisopropylamide in THF under nitrogen gas for 2 hours followed by treatment with benzyl bromide to provide the highest percentage yield of product (entry 1 and 3 in Table 25). Hence, synthesis of the other optically active form and substitution with benzyl bromide were synthesized *via* this condition. The products which can be no isolated the both diastereomeric forms were purified by flash column chromatography (EtOAc/Acetone/hexane = 1:1:8 as eluent) as shown in Scheme 23.

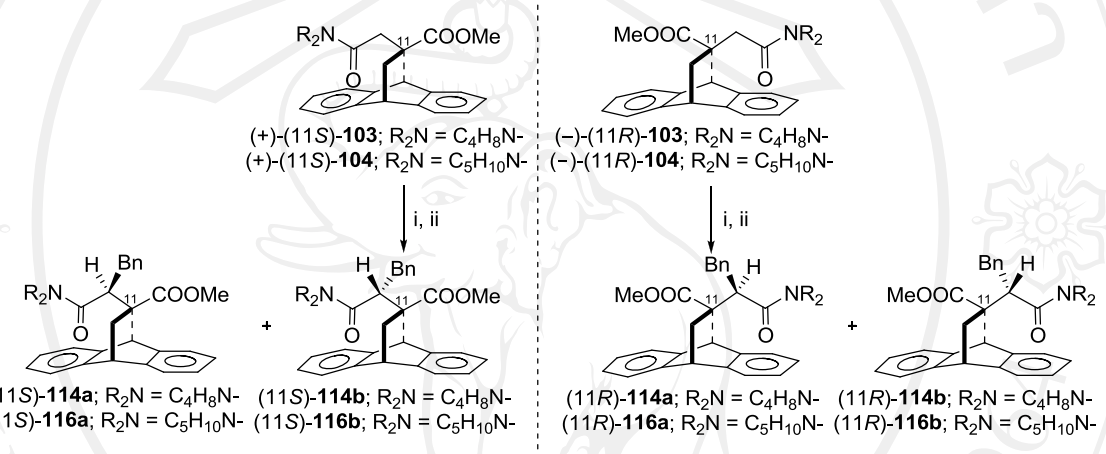

Scheme 23 Synthesis of optically active benzyl amide–anthracene adducts (11*S*)-**114**, (11*R*)-**114**, (11*S*)-**116**, and (11*R*)-**116**. *Reagents and conditions*: (i) 1.2 equiv LDA, THF, –78 °C to 0 °C, N_2, 2 h; (ii) 2.0 equiv BnBr, –78 °C to rt, N_2, overnight.

From the NMR spectral of the diastereomeric adducts **114** (Figure 7), they were found that the substitution reaction with benzyl bromide of pyrrolidinyl amide–anthracene adducts (11*S*)-**103** gave adduct (11*S*)-**114a** as major products and adduct (11*S*)-**114b** as minor products in the ratio of 2.8:1 which were mainly calculated from ^{1}H-NMR spectral. The substitution reaction with benzyl bromide of pyrrolidinyl amide–anthracene adducts (11*R*)-**103** gave adduct (11*R*)-**114a** as major products and adduct (11*R*)-**114b** as minor products in the ratio of 1.7:1. Their ^{1}H-NMR spectrum showed the proton H_y of adducts **114a** as singlet at δ 4.70 ppm which was higher field than the proton H_y of adducts **114b**. This may be the result of deshielding effect of the aromatic nuclei. The proton H_x of adducts **114a** were shown at δ 4.33 ppm which

was lower field than the proton H_x of adducts **114b**. These ^{1}H-NMR signals pattern are similar at ^{1}H-NMR signals pattern of diastereomeric β-ketodiester which were reported by Jongkol and co-worker in 2011.[32] For these reasons, the configuration of major products **114a** could be proposed that the orientation of the proton H_c occupied far from the anthracene ring. The structure of benzyl pyrrolidinyl amide–anthracene adducts (11*S*)-**114a**, (11*S*)-**114b**, (11*R*)-**114a** and (11*R*)-**114b** could be confirmed by MM2 force field calculations for energy minimization from modeling program ChemBio3D Ultra 11.0 program as depicted in Figure 8.

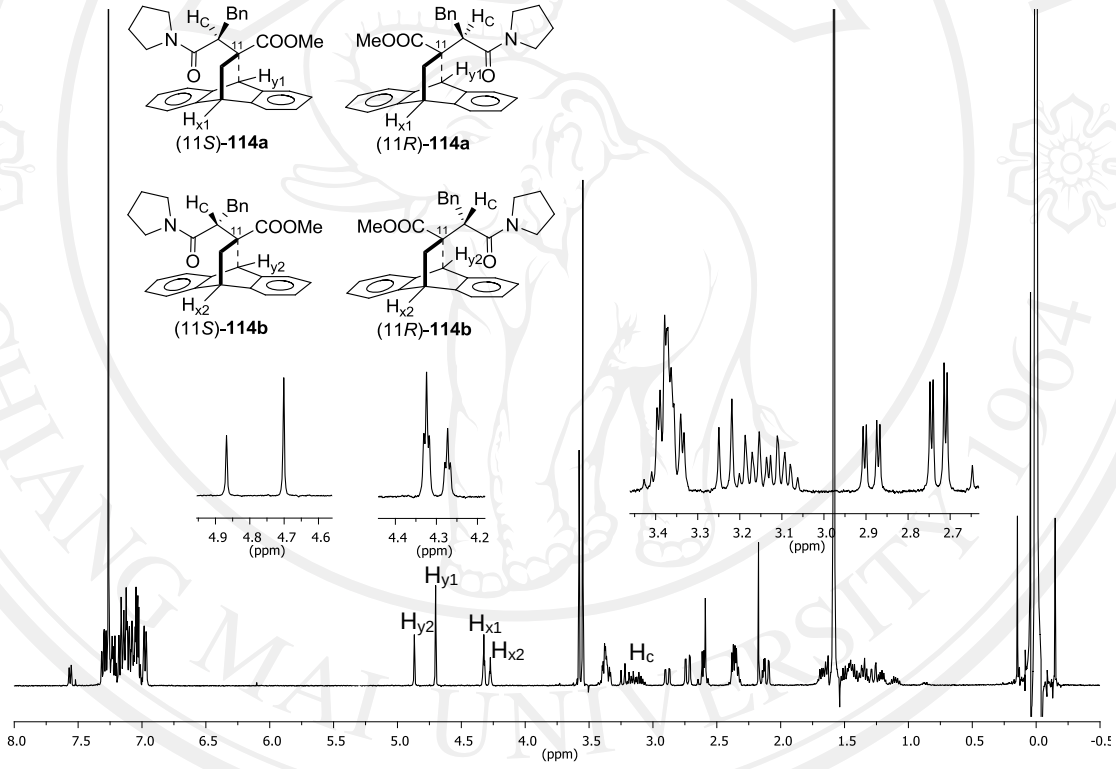

Figure 7 ^{1}H-NMR spectral data of benzyl pyrrolidinyl amide–anthracene adducts (11*S*)-**114a**, (11*S*)-**114b**, (11*R*)-**114a** and (11*R*)-**114b**

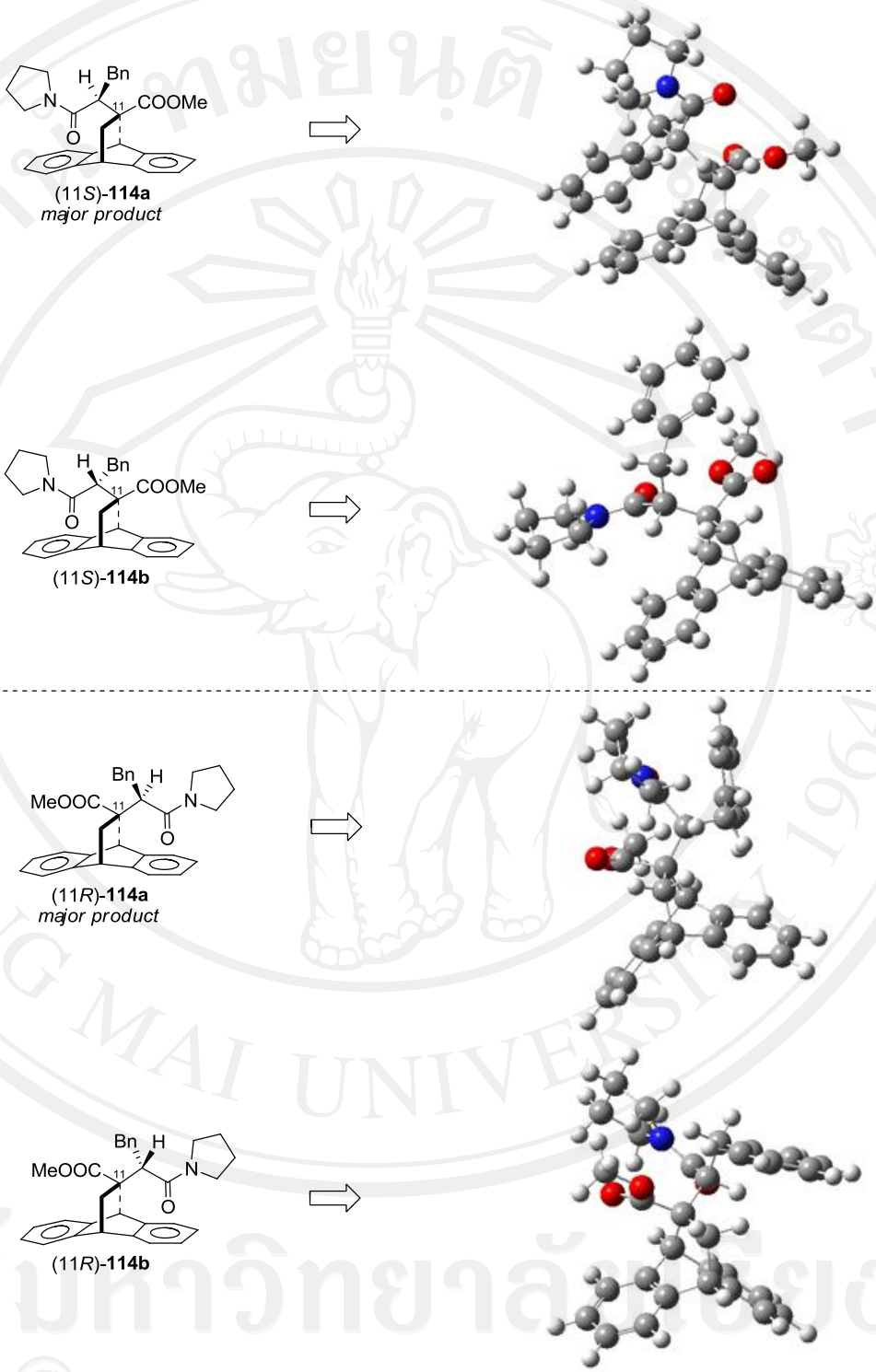

Figure 8 3D structure conformation of benzyl pyrrolidinyl amide–anthracene adducts (11*S*)-**114a**, (11*S*)-**114b**, (11*R*)-**114a** and (11*R*)-**114b** were generated by MM2 force field calculations for energy minimization from modeling program Chem3D Ultra 11.0 and GaussView 3.09 program

From the NMR spectral of the both diastereomeric adducts **116** (Figure 9), they were found that the substitution reaction with benzyl bromide of the both optically active piperidinyl amide–anthracene adducts **104** gave adducts **116a** and adducts **116b** in the ratio of 1:1 which were mainly calculated from ^{1}H-NMR spectral. Their ^{1}H-NMR spectrum showed the proton H_y of adducts **116a** as singlet at δ 4.59 ppm which was higher field than the proton H_y of adducts **116b**. This may be the result of deshielding effect of the aromatic nuclei. The proton H_x of adducts **114a** were shown at δ 4.43 ppm which was lower field than the proton H_x of adducts **114b**. These ^{1}H-NMR signals pattern are similar at ^{1}H-NMR signals pattern of diastereomeric β-ketodiester which were reported by Jongkol and co-worker in 2011.[32] For these reasons, the configuration of adducts **114a** could be proposed that the orientation of the proton H_c occupied far from the anthracene ring. The structure of adducts (11*S*)-**116a**, (11*S*)-**116b**, (11*R*)-**116a** and (11*R*)-**116b** could be confirmed by MM2 force field calculations for energy minimization from modeling program ChemBio3D Ultra 11.0 program as depicted in Figure 10.

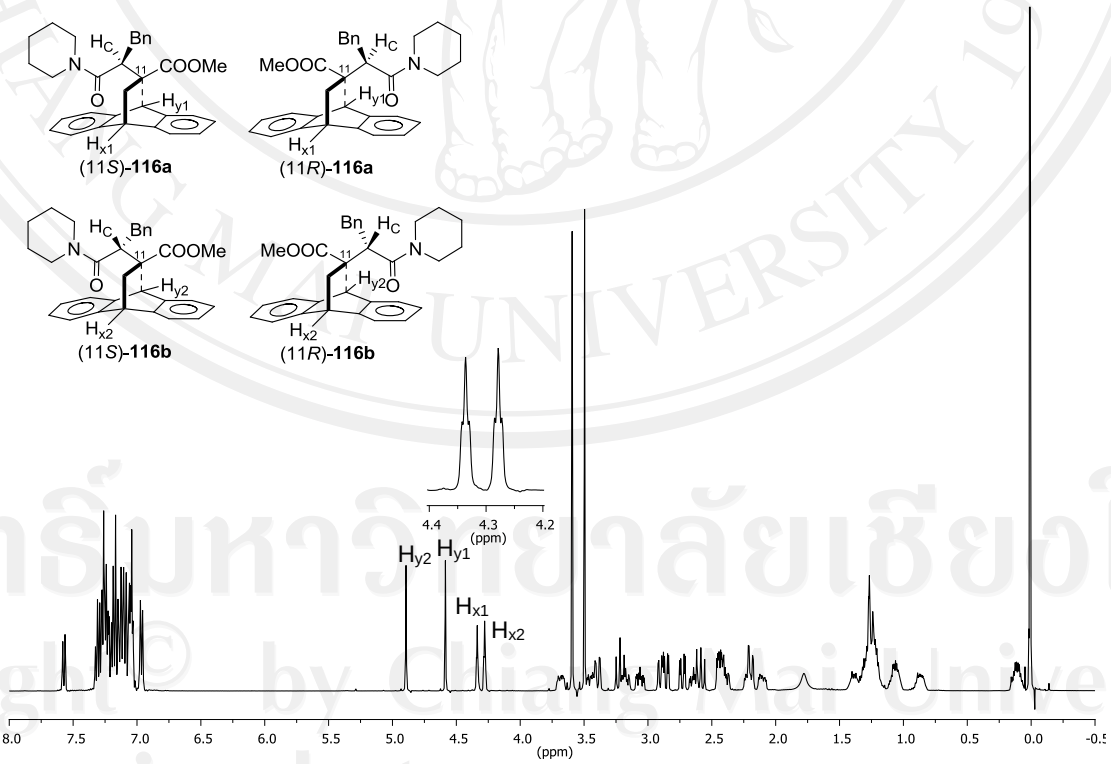

Figure 9 ^{1}H-NMR spectral data of benzyl piperidinyl amide–anthracene adducts (11*S*)-**116a**, (11*S*)-**116b**, (11*R*)-**116a** and (11*R*)-**116b**

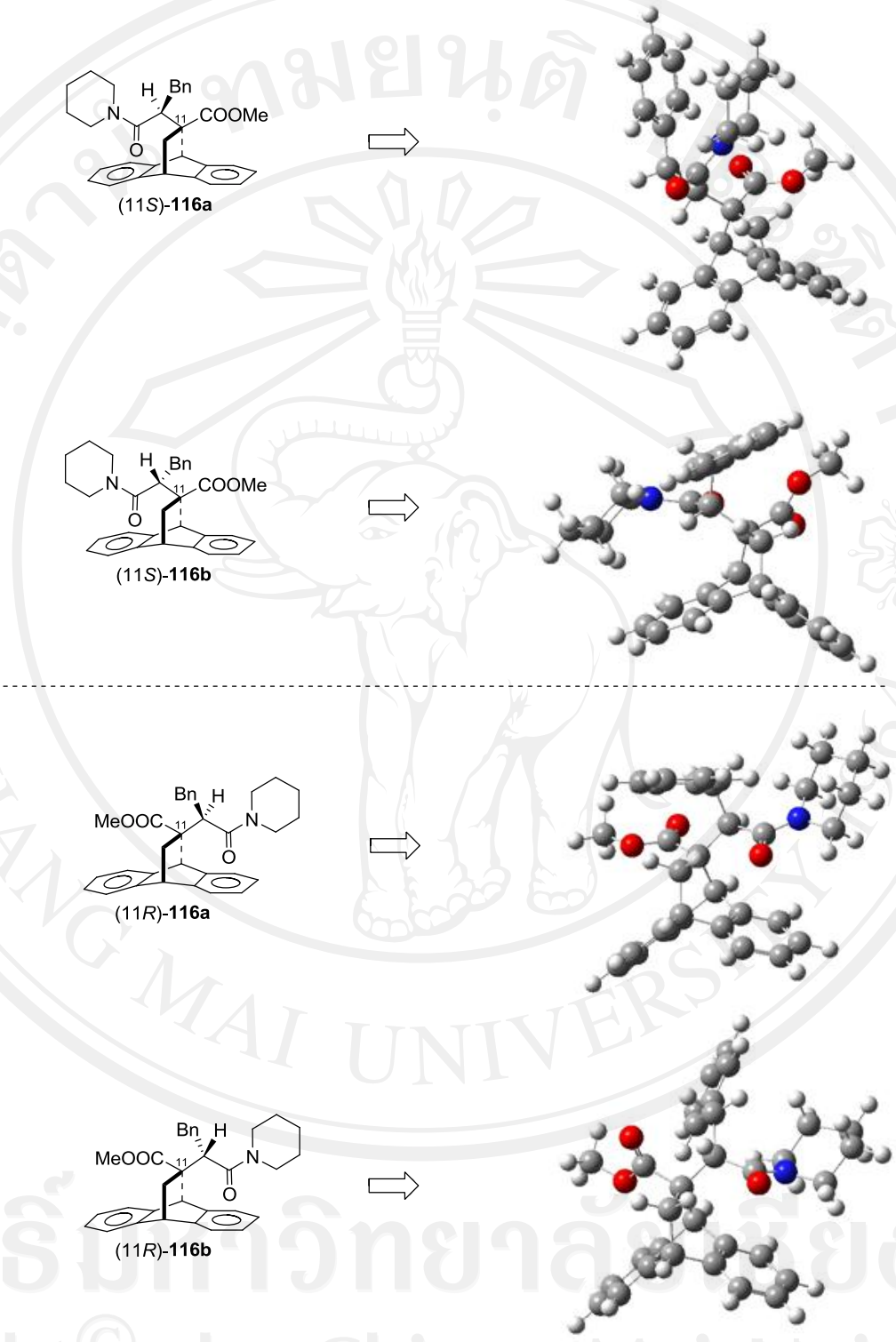

Figure 10 3D structure conformation of benzyl piperidinyl amide–anthracene adducts (11*S*)-**116a**, (11*S*)-**116b**, (11*R*)-**116a** and (11*R*)-**116b** were generated by MM2 force field calculations for energy minimization from modeling program Chem3D Ultra 11.0 and GaussView 3.09 program

Next step, the benzyl amide–anthracene adducts (11*R*)-**114** and (11*R*)-**116** were used as a model compounds for studying of disubstituted reactions with benzyl bromide. They were studied by varying the stoichiometric equivalent of lithium diisopropylamide (LDA) and addition of *N*,*N*,*N*′,*N*′-tetramethylethane-1,2-diamine (TMEDA) as cosolvent. The results are shown in Table 26. The adducts (11*S*)-**121** and (11*S*)-**122** were not observed in these reactions, due to steric effect of bulky groups which are anthracene ring, benzyl group and pyrrolidine ring or piperidine ring. Also, anion of these adducts cannot attack at benzyl bromide.

Table 26 Optimization of synthetic dibenzylamide anthracene adducts (11*S*)-**121** and (11*S*)-**122**

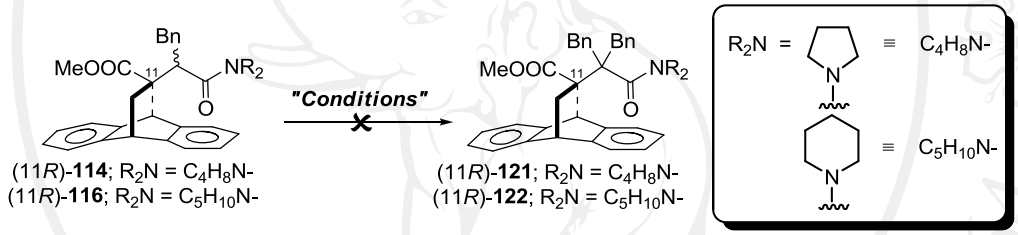

Entry	R_2N	Conditions	Results
1	C_4H_8N-	i) 1.2 equiv LDA, THF, –78 °C to 0 °C, N_2, 2 h ii) 2.0 equiv BnBr, –78 °C to rt, N_2, overnight	Recovered (11*R*)-**114**
2		i) 2.0 equiv LDA, THF, –78 °C to 0 °C, N_2, 2 h ii) 2.0 equiv BnBr, –78 °C to rt, N_2, overnight	Recovered (11*R*)-**114**
3		i) 1.2 equiv LDA, THF, –78 °C to 0 °C, N_2, 2 h ii) 1.2 equiv TMEDA, –78 °C, 15 min iii) 2.0 equiv BnBr, –78 °C to rt, N_2, overnight	Recovered (11*R*)-**114**
4	$C_5H_{10}N$-	i) 1.2 equiv LDA, THF, –78 °C to 0 °C, N_2, 2 h ii) 2.0 equiv BnBr, –78 °C to rt, N_2, overnight	Recovered (11*R*)-**116**
5		i) 2.0 equiv LDA, THF, –78 °C to 0 °C, N_2, 2 h ii) 2.0 equiv BnBr, –78 °C to rt, N_2, overnight	Recovered (11*R*)-**116**
6		i) 1.2 equiv LDA, THF, –78 °C to 0 °C, N_2, 2 h ii) 1.2 equiv TMEDA, –78 °C, 15 min iii) 2.0 equiv BnBr, –78 °C to rt, N_2, overnight	Recovered (11*R*)-**116**

3.3.2 Synthesis of diastereomeric methyl(piperidinyl or pyrrolidinyl) amide–anthracene adducts ((11*S*)-115, (11*R*)-115, 11(*S*)-117 and (11*R*)-117)

From Scheme 24, Synthesis of the both optically active methyl amide–anthracene adducts (11*S*)-**115**, (11*R*)-**115**, 11(*S*)-**117** and (11*R*)-**117** were synthesized *via* the best conditions of substitution reaction with benzyl bromide in the table 25 (entry 1 and 3 in Table 25).

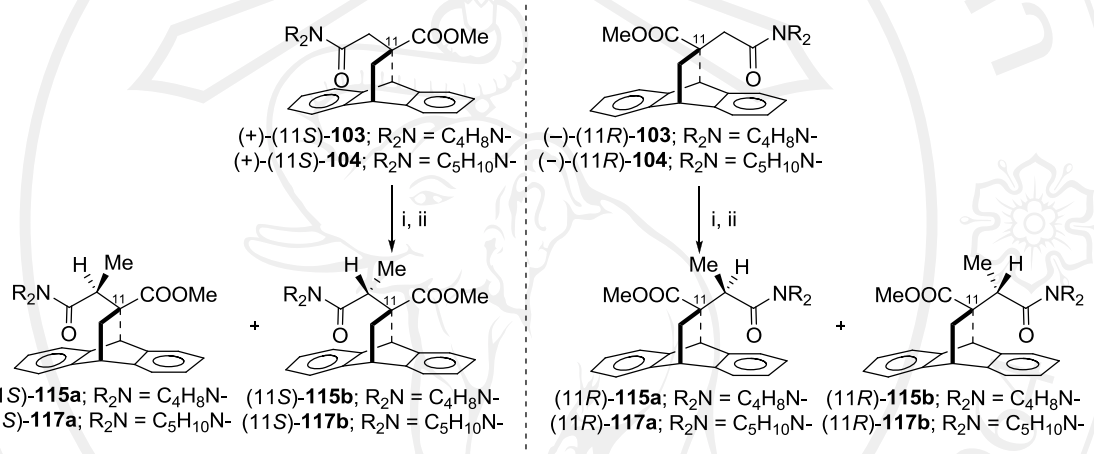

Scheme 24 Synthesis of optically active methyl amide–anthracene adducts (11*S*)-**115**, (11*R*)-**115**, (11*S*)-**117**, and (11*R*)-**117**. *Reagents and conditions*: (i) 1.2 equiv LDA, THF, –78 °C to 0 °C, N_2, 2 h; (ii) 2.0 equiv MeI, –78 °C to rt, N_2, overnight.

The optically active amide–anthracene adducts reacted with 1.2 equivalents of lithium diisopropylamide in THF under nitrogen gas for 2 hours followed by treating with methyl iodide at –78 °C to room temperature for overnight. After that, the reaction mixture was worked up with 10% hydrochloric acid. The products and starting material could be not purified by flash column chromatography.

From the NMR spectral of the diastereomeric adducts **115** (Figure 11), they were found that the substitution reaction with benzyl bromide of piperidinyl amide–anthracene adducts (11*S*)-**103** gave adduct (11*S*)-**115a** and adduct (11*S*)-**115b** in the ratio of 1:1 which were mainly calculated from ^{1}H-NMR spectral. The substitution reaction with benzyl bromide of piperidinyl amide–anthracene adduct (11*R*)-**103** gave adduct (11*R*)-**115a** as major products and adduct (11*R*)-**115b** as minor products in the

ratio of 1.5:1. Their ^{1}H-NMR spectrum showed the proton H_y of adducts **115a** as singlet at δ 4.64 ppm which was higher field than the proton H_y of adducts **114b**. This may be the result of deshielding effect of the aromatic nuclei. These ^{1}H-NMR signals pattern are similar at ^{1}H-NMR signals pattern of diastereomeric β-ketodiester which were reported by Jongkol and co-worker in 2011.[32] For these reasons, the configuration **115a** could be proposed that the orientation of the proton H_c occupied far from the anthracene ring. The structure of methyl pyrrolidinyl amide–anthracene adducts (11*S*)-**115a**, (11*S*)-**115b**, (11*R*)-**115a** and (11*R*)-**115b** could be confirmed by MM2 force field calculations for energy minimization from modeling program ChemBio3D Ultra 11.0 program as depicted in Figure 12.

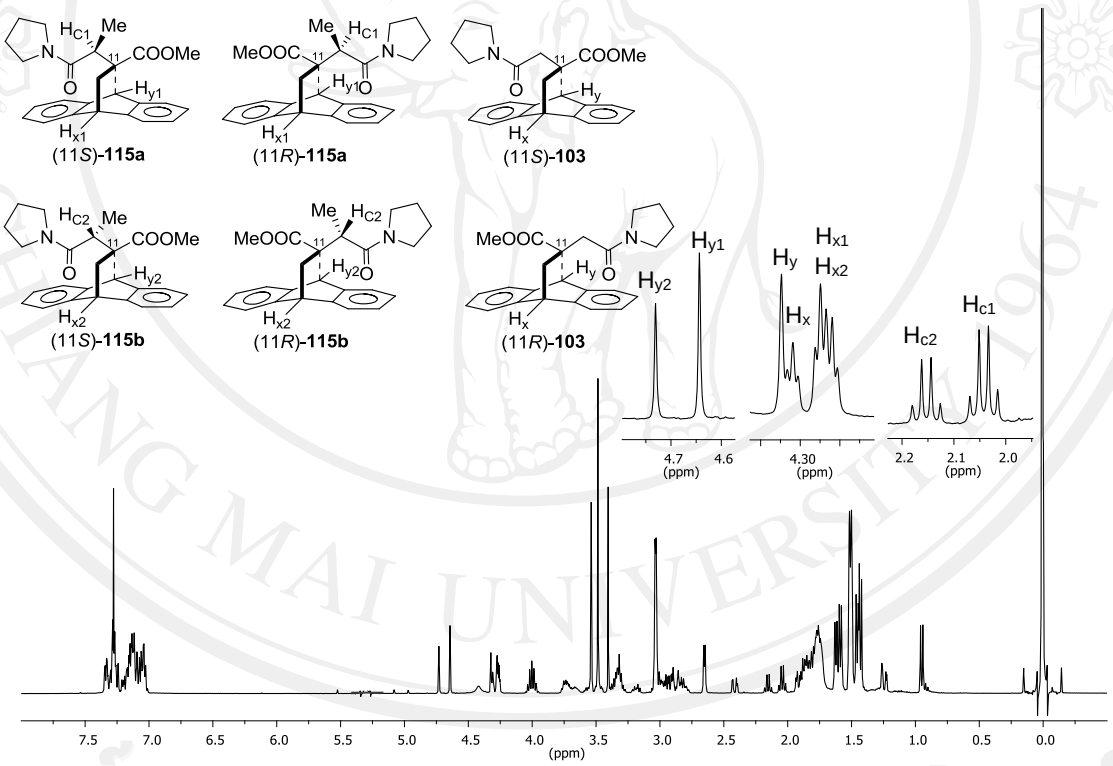

Figure 11 ^{1}H-NMR spectral data of methyl pyrrolidinyl amide–anthracene adducts (11*S*)-**115a**, (11*S*)-**115b**, (11*R*)-**115a** and (11*R*)-**115b**

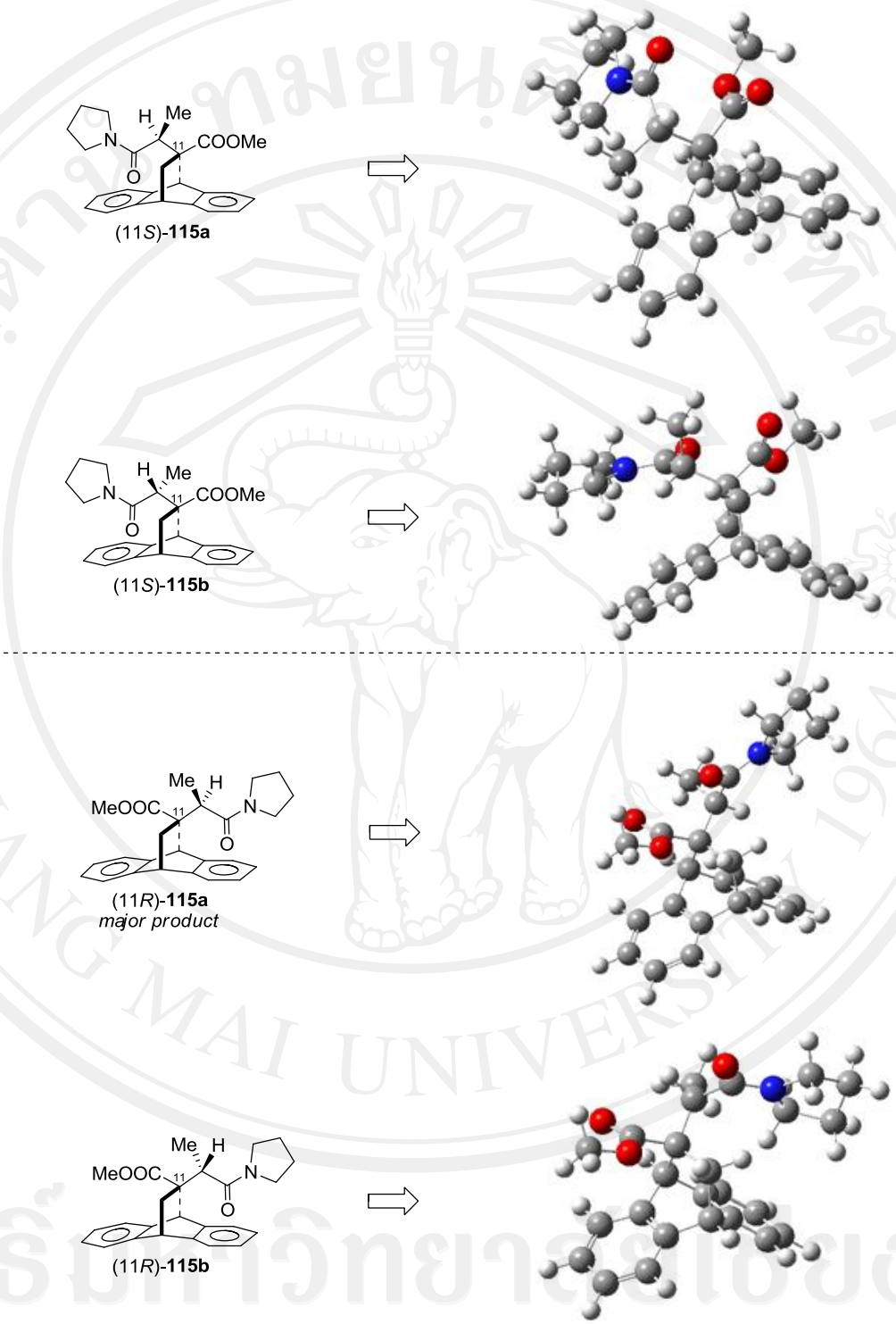

Figure 12 3D structure conformation of benzyl pyrrolidinyl amide–anthracene adducts (11*S*)-**115a**, (11*S*)-**115b**, (11*R*)-**115a** and (11*R*)-**115b** were generated by MM2 force field calculations for energy minimization from modeling program Chem3D Ultra 11.0 and GaussView 3.09 program

From the NMR spectral of the both diastereomeric adducts **117** (Figure 13), they were found that the substitution reaction with benzyl bromide of the both optically active piperidinyl amide–anthracene adducts **104** gave adducts **117b** as major products and adducts **117a** as minor products in the ratio of 2:1 which were mainly calculated from ^{1}H-NMR spectral. Their ^{1}H-NMR spectrum showed the proton H_y of adducts **117b** as singlet at δ 4.62 ppm which was lower field than the proton H_y of adducts **117a**. This may be the result of deshielding effect of the aromatic nuclei. These ^{1}H-NMR signals pattern are similar at ^{1}H-NMR signals pattern of diastereomeric β-ketodiester which were reported by Jongkol and co-worker in 2011.[32] For these reasons, the configuration of adducts **117a** could be proposed that the orientation of the proton H_c occupied near the anthracene ring. The structure of methyl piperilinyl amide–anthracene adducts (11*S*)-**117a**, (11*S*)-**117b**, (11*R*)-**117a** and (11*R*)-**117b** could be confirmed by MM2 force field calculations for energy minimization from modeling program ChemBio3D Ultra 11.0 program as depicted in Figure 14.

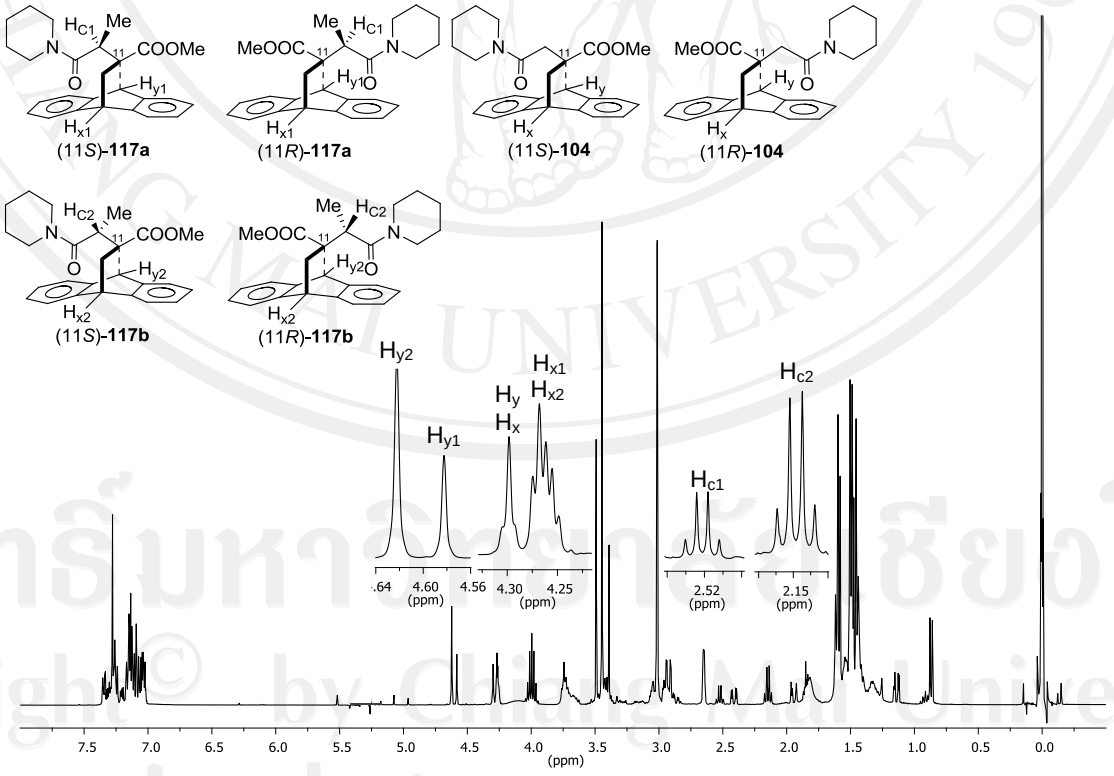

Figure 13 ^{1}H-NMR spectral data of benzyl pyrrolidinyl amide–anthracene adducts (11*S*)-**117a**, (11*S*)-**117b**, (11*R*)-**117a** and (11*R*)-**117b**

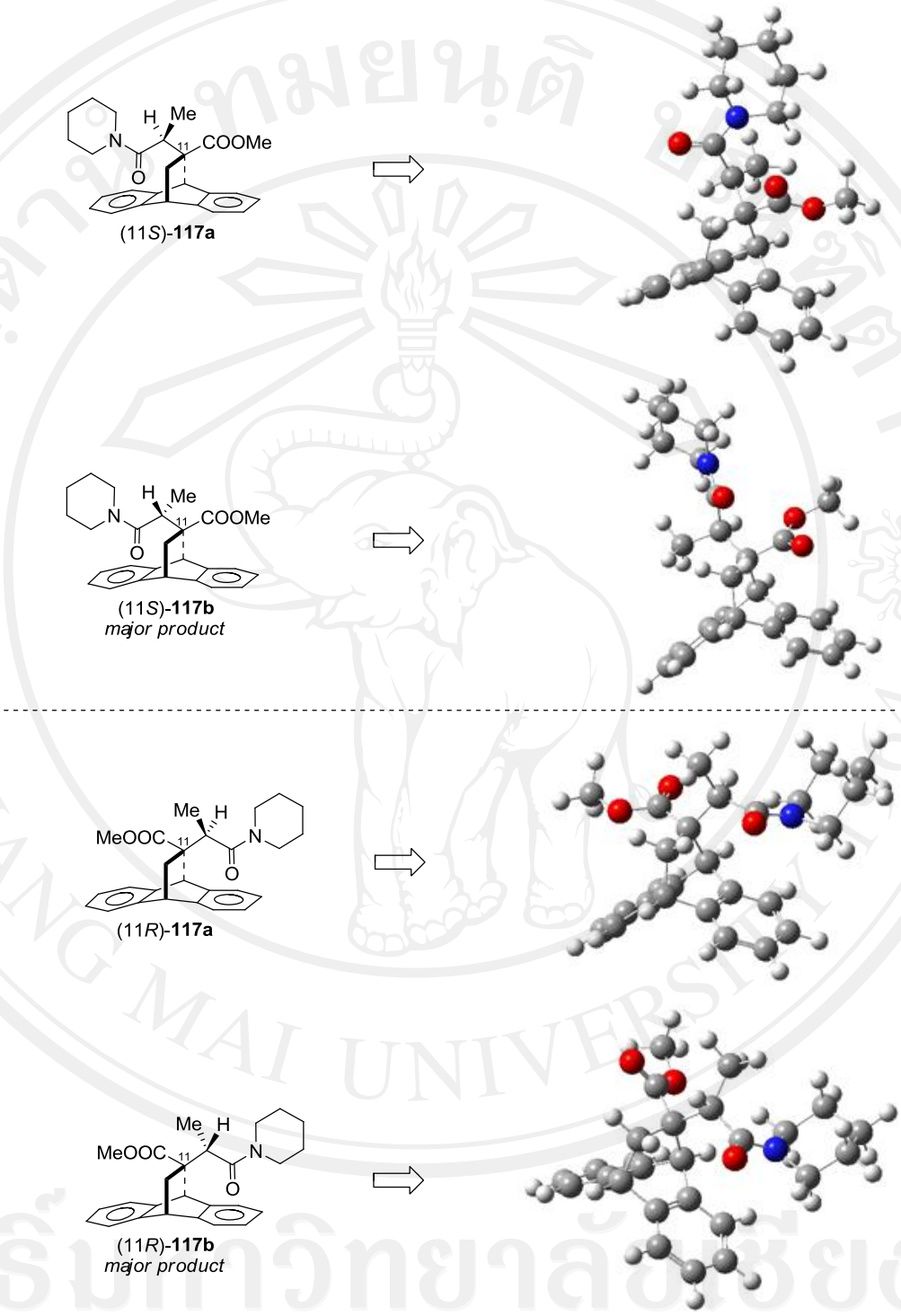

Figure 14 3D structure conformation of benzyl piperidinyl amide–anthracene adducts (11*S*)-**117a**, (11*S*)-**117b**, (11*R*)-**117a** and (11*R*)-**117b** were generated by MM2 force field calculations for energy minimization from modeling program Chem3D Ultra 11.0 and GaussView 3.09 program

3.4 Synthesis of optically active amide spiro–lactone anthracene adducts (+)-(4′*S*,11*R*)-107a, (4′*R*,11*R*)-107b, (+)-(4′*S*,11*R*)-108a and (4′*R*,11*R*)-108b

The optically active amide spiro–lactone adducts **107a** and **108a** were synthesized from optically active pyrrolidinyl amide–anthracene adduct (+)-(11*S*)-**103** and piperidinyl amide–anthracene adduct (+)-(11*S*)-**104** *via* tandem aldol-lactonization reactions, respectively. The amide–anthracene adducts (+)-(11*S*)-**103** and (+)-(11*S*)-**104** reacted with lithium diisopropylamide (LDA, 1.2 equiv) in THF at −78 °C to 0 °C for 2 hour to obtain enolate anions **A** and **B** (Scheme 25). And then, these enolate anions were treated with benzophenone at −78 °C to room temperature for overnight followed by 10% hydrochloric acid work up. The crude products were purified by flash column chromatography (CH_2Cl_2/EtOAc/hexane = 1:2:7 as eluent).

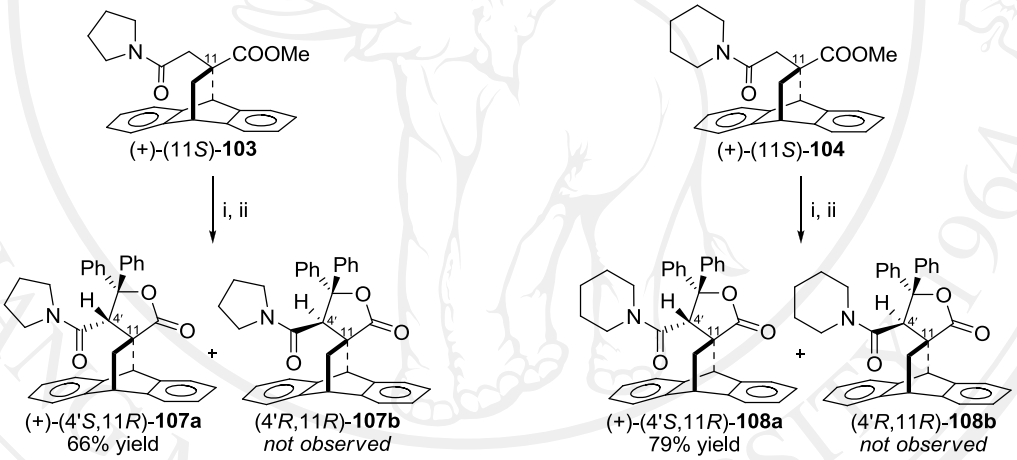

a) Synthesis of pyrrolidinyl spiro–lactone anthracene adducts

b) Synthesis of piperidinyl spiro–lactone anthracene adducts

Scheme 25 Synthesis of optically active pure amide spiro–lactone anthracene adducts (+)-(4′*S*,11*R*)-**107a**, (4′*R*,11*R*)-**107b**, (+)- (4′*S*,11*R*)-**108a** and (4′*R*,11*R*)-**108b** *via* tandem aldol-lactonization reactions. *Reagents and conditions*: (i) 1.2 equiv LDA, THF, −78 °C to 0 °C, N_2, 2 h; (ii) 1.2 equiv benzophenone, −78 °C to rt, N_2, overnight.

In case of pyrrolidinyl spiro–lactone anthracene adduct, the optically active pure pyrrolidinyl spiro–lactone anthracene adduct (+)-(4′*S*,11*R*)-**107a** was obtained in 66% yield, $[\alpha]_{589}^{28.9}$ = +87.44° (*c* = 0.215, $CHCl_3$) but conformation of adduct

(4′*R*,11*R*)-**107b** was be not observed in this reaction as shown in Scheme 25a. In addition, the optically active pure pyrrolidinyl spiro–lactone anthracene adduct (+)-(4′*S*,11*R*)-**108a** was obtained in 79% yield, $[\alpha]_{589}^{29.0}$ = +98.43° (*c* = 0.254, $CHCl_3$) but conformation of adduct (4′*R*,11*R*)-**108b** was be not observed in this reaction as shown in Scheme 25b.

The orientation of H_c on carbon-4′ can be described *via* the chair–like transition state models **C** and **D** as shown in Scheme 26. The transition state **D** had more steric repulsion between the phenyl group and the anthracene ring than the transition state **C**. Also, the transition state **C** would lead to the product (+)-(4′*S*,11*R*)-**107a** and product (+)-(4′*S*,11*R*)-**108a**. In contrast, the transition state **D** would lead to the conformation of (4′*R*,11*R*)-**107b** and (4′*R*,11*R*)-**108b** which were not observed in these reactions.

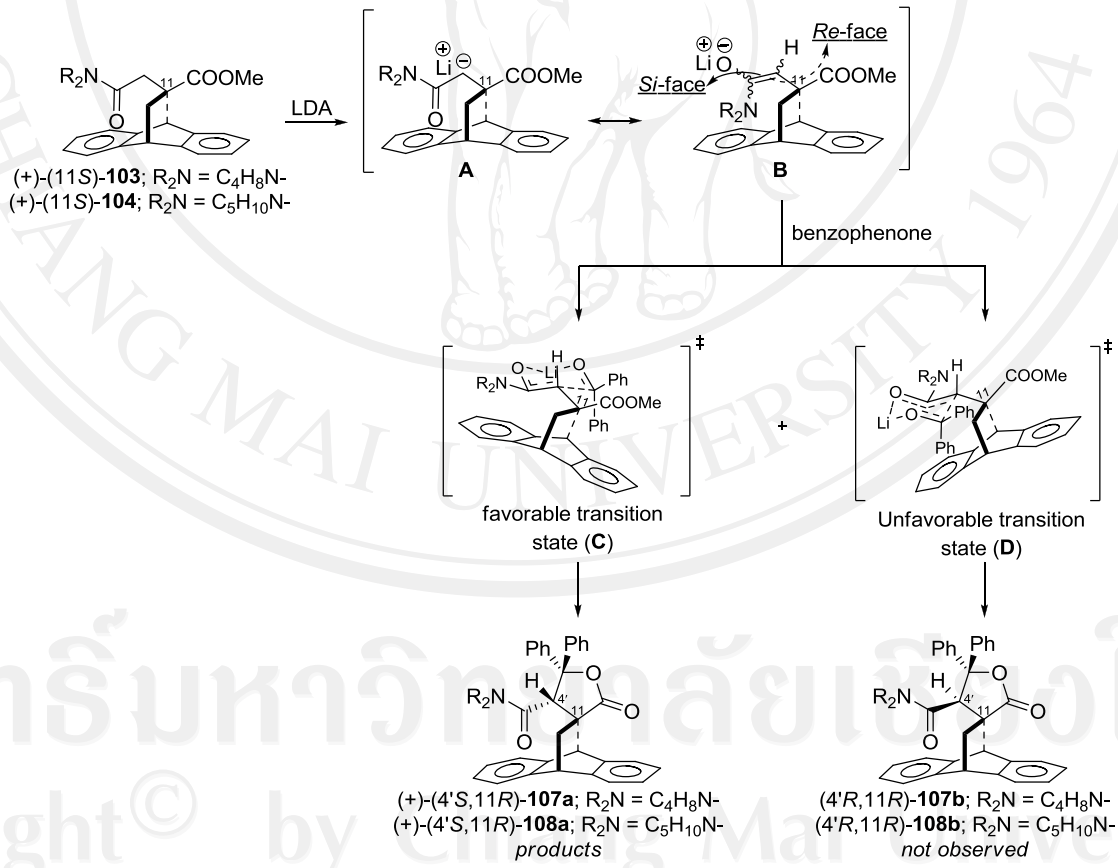

Scheme 26 Proposed mechanism of diastereoselective tandem aldol-lactonization reactions of the amide spiro–lactone anthracene adducts.

The structure and stereochemistry of pyrrolidinyl spiro–lactone anthracene adduct (+)-(4′*S*,11*R*)-**107a** can be confirmed by NMR and NOE experiment. The signal of proton H_a, H_b and H_x appeared at 1.52, 1.56 and 4.13 ppm (*ABX* system, (*J* = 13.6, 2.3 and 2.0 Hz), proton H_c at 3.26 ppm as singlet, proton H_y at 5.11 ppm as singlet and aromatic protons at 6.95–7.49 ppm as multiplet. In addition, the signal of protons on pyrrolidine ring, which are one proton on methylene C-9′ appeared at 1.49–1.35 ppm as multiplet, two protons methylene C-8′ and one proton on methylene C-9′ appeared at 1.63–1.77 ppm as multiplet, two proton on methylene C-7′ appeared at 2.23–2.34 and 2.97–3.13 ppm as multiplet and two proton of methylene C-10′ appeared at 2.63–2.74 and 3.21–3.37 ppm as multiplet. The correlation protons on H_a, H_b, H_c and protons on pyrrolidine ring were confirmed by COSY correlation. Besides, HMQC correlation showed that H_c correlated with methylene C-4′ and protons on pyrrolidine ring correlated with C-7′, C-8′, C-9′ and C-10′. HMBC correlation showed that proton H_c correlated with quaternary C-6′.

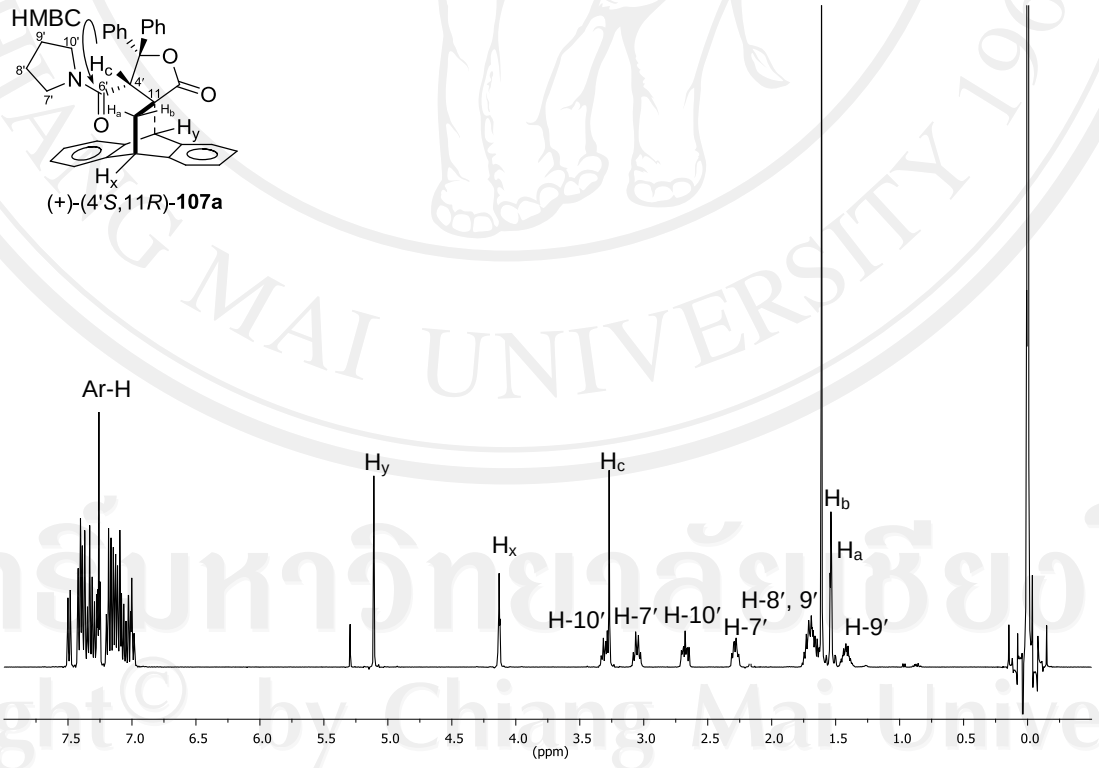

Figure 15 ^{1}H-NMR spectral data of pyrrolidinyl spiro–lactone anthracene adduct (+)-(4′*S*,11*R*)-**107a** (Plain arrow was HMBC correlation)

From NOE experiment, it showed that the proton H_c enhanced with the proton H_a but no NOE effect with the proton H_y. Hence, the orientation of the proton H_c is on the upper face and *syn*- with the proton H_a but *anti*- with the proton H_y. Besides, the structure of pyrrolidinyl spiro–lactone anthracene adduct (+)-(4′*S*,11*R*)-**107a** could be confirmed by MM2 force field calculations for energy minimization from modeling program ChemBio3D Ultra 11.0 program as depicted in Figure 16. Result of adduct (+)-(4′*S*,11*R*)-**107a** showed that the distance form H_c to H_a and H_c to H_y are 2.17 and 3.60 Å, respectively. The results from computational calculation are in agreement with the NOE results.

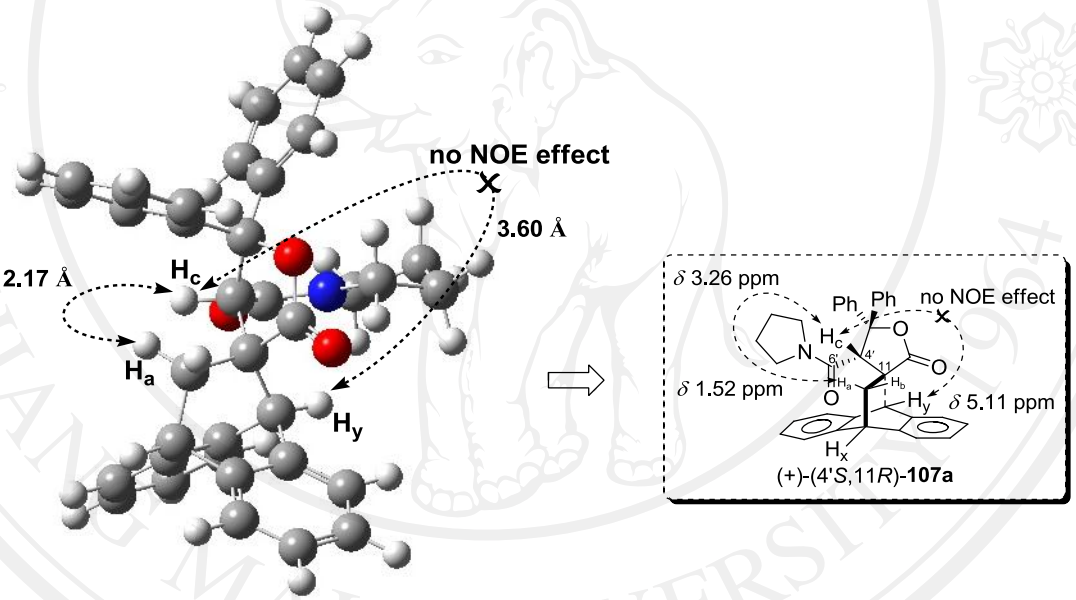

Figure 16 3D structure conformation of pyrrolidinyl spiro–lactone anthracene adduct (+)-(4′*S*,11*R*)-**107a** was generated by MM2 force field calculations for energy minimization from modeling program Chem3D Ultra 11.0 and GaussView 3.09 program with the observed NOE correlations (arrows)

Additionally, The structure of piperidinyl spiro–lactone anthracene adduct (+)-(4′*S*,11*R*)-**108a** was confirmed by NMR technique. The ^{1}H-NMR spectrum of this adduct is depicted in Figure 17. The signal of proton H_a, H_b and H_x appeared at 1.50, 1.55 and 4.09 ppm (*ABX* system, (*J* = 13.1, 3.1 and 2.4 Hz), proton H_c at 3.56 ppm as singlet, proton H_y at 5.04 ppm as singlet and aromatic protons at 6.38–7.81

ppm as multiplet. Furthermore, the signal of protons on piperidine ring, which are six protons on methylene C-8′, methylene C-9′ and methylene C-10′ appeared at 0.81-0.96, 1.17–1.31 and 1.32–1.46 ppm as multiplet, two protons methylene C-7′ appeared at 2.63–2.75 and 2.78–2.90 ppm as multiplet and two proton of methylene C-11′ appeared at 3.01–3.12 and 3.16–3.29 ppm as multiplet. The correlation protons on H_a, H_b, H_c and protons on piperidine ring were confirmed by COSY correlation. Moreover, HMQC correlation showed that H_c correlated with methylene C-4′ and protons on piperidine ring correlated with C-7′, C-8′, C-9′, C-10′ and C-11′. HMBC correlation showed that proton H_c correlated with quaternary C-6′.

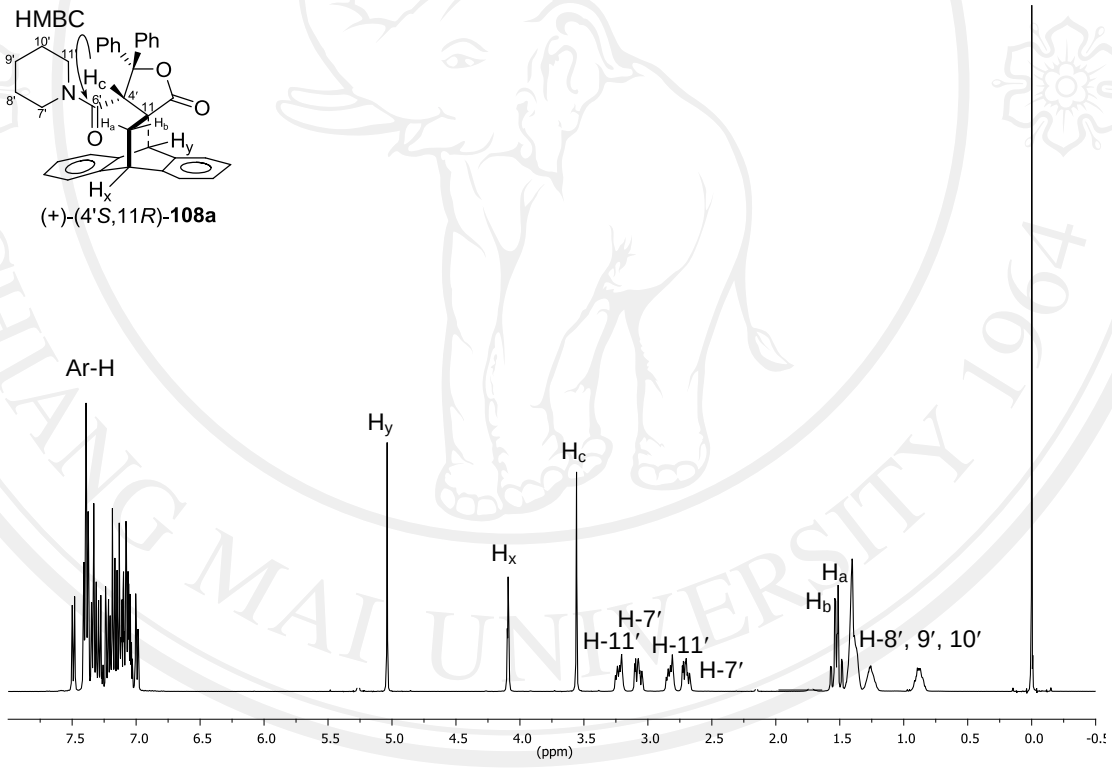

Figure 17 ^{1}H-NMR spectral data of piperidinyl spiro–lactone anthracene adduct (+)-(4′*S*,11*R*)-**108a** (Plain arrow was HMBC correlation)

The stereochemistry of piperidinyl spiro–lactone anthracene adduct can be confirmed by NOE technique, it showed that irradiation of the proton H_c gave a NOE effect on the proton H_a but no NOE effect on the proton H_y. Consequently, the orientation of the proton H_c is on the upper face and *syn*- with the proton H_a but *anti*- with the proton H_y. Furthermore, the structure of piperidinyl spiro–lactone anthracene

adduct (+)-(4′*S*,11*R*)-**108a** could be confirmed by MM2 force field calculations for energy minimization from modeling program ChemBio3D Ultra 11.0 program as depicted in Figure 18. Result of adduct (+)-(4′*S*,11*R*)-**108a** indicated that the distance form H_c to H_a and H_c to H_y are 2.17 and 3.60 Å, respectively. The results from computational calculation are in agreement with the NOE results.

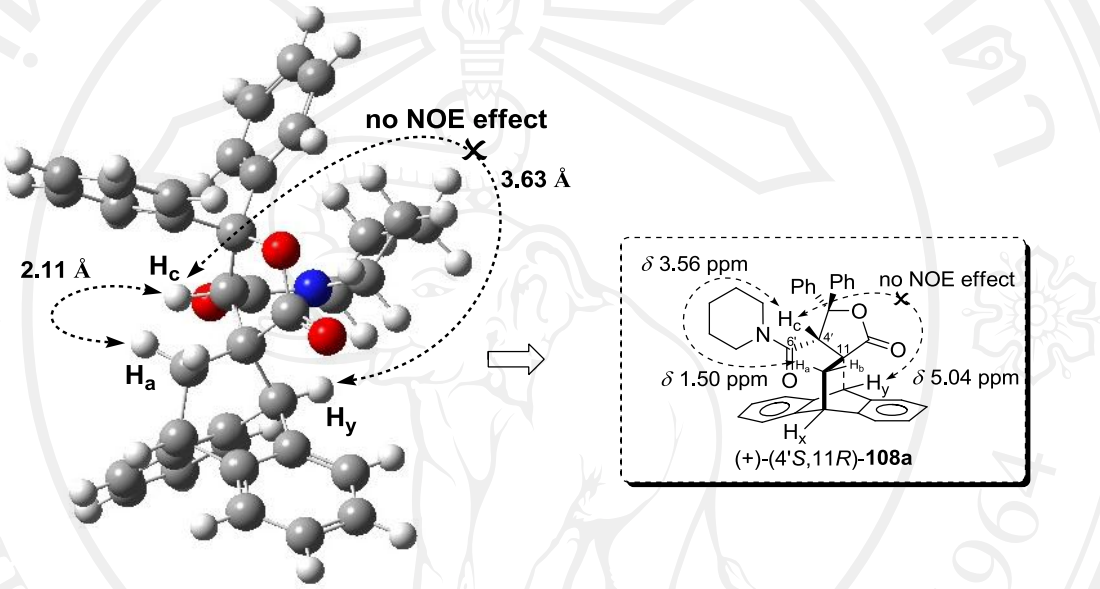

Figure 18 3D structure conformation of piperidinyl spiro–lactone anthracene adduct (+)-(4′*S*,11*R*)-**108a** was generated by MM2 force field calculations for energy minimization from modeling program Chem3D Ultra 11.0 and GaussView 3.09 program with the observed NOE correlations (arrows)

3.5 Preparation of *N,O* heteroatoms TADDOLs–anthracene adducts *via* reduction reaction of amide–anthracene adducts and amide spiro–lactone anthracene adducts

Importantly, the reduction reaction of amide–anthracene adducts and amide spiro–lactone anthracene adducts are the last step for synthesis of *N,O* heteroatoms TADDOLs–anthracene adducts. They were studied by various stoichiometric equivalent of lithium aluminium hydride (LAH) and reaction times using pyrrolidinyl amide–anthracene adduct (+)-(11*S*)-**103**, piperidinyl amide–anthracene adduct (+)-(11*S*)-**104**, pyrrolidinyl spiro–lactone anthracene adduct (+)-(4′*S*,11*R*)-**107a** and

piperidinyl spiro–lactone anthracene adduct (+)-(4′*S*,11*R*)-**108a** as model compounds, respectively. The schematic of target *N*,*O* heteroatoms TADDOLs–anthracene adducts is shown in Scheme 27.

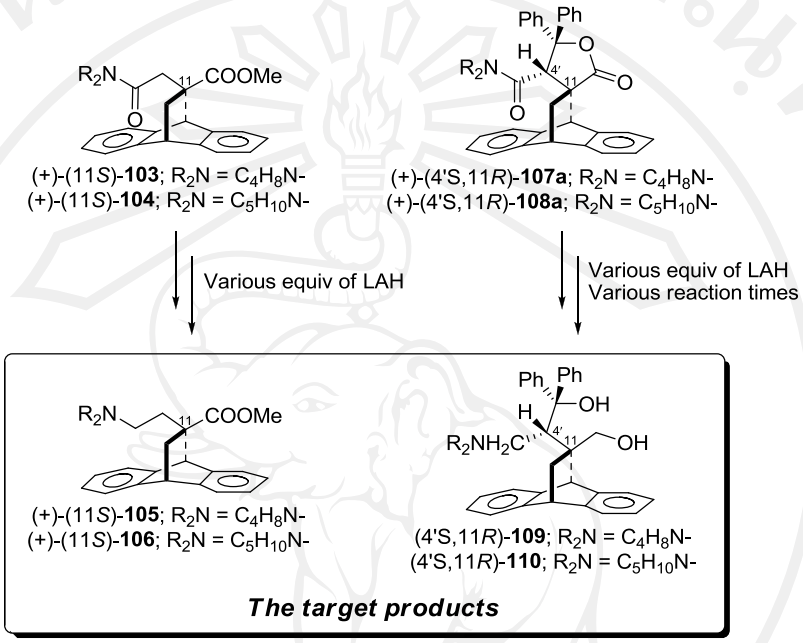

Scheme 27 The target product, *N*,*O* heteroatoms TADDOLs–anthracene adducts.

3.5.1 Reduction reaction of both enantiomerically pure pyrrolidinyl amide–anthracene adducts (+)-(11*S*)-103 and (–)-(11*S*)-103

At the beginning, synthesis of (11*S*)-11-hydroxymethylene-11-(2′′-pyrrolidinyl)-9,10-dihydro-9,10-ethanoanthracene was studied by various stoichiometric equivalent of lithium aluminium hydride (LAH). The reduction reactions of pyrrolidinyl amide–anthracene adduct (+)-(11*S*)-**103** which were used as model reaction are shown in Table 27.

Table 27 Optimization of conditions for reduction reaction of pyrrolidinyl amide–anthracene adduct (+)-(11*S*)-**103**

Table 27 Optimization of conditions for reduction reaction of pyrrolidinyl amide–anthracene adduct (+)-(11*S*)-**103** (continued)

Entry	Conditions	Yield (%)[a]	Conversion (%)
1	5.0 equiv LAH, THF, reflux, N_2, overnight	56	100
2	5.0 equiv LAH, THF, –78 °C to rt, N_2, 2 days	64	100
3	10.0 equiv LAH, THF, –78 °C to rt, N_2, 2 days	50	100
4	15.0 equiv LAH, THF, –78 °C to rt, N_2, 2 days	42	100

[a] Isolated yield

From Table 27, Entry 1-4 demonstrated the reduction reaction of pyrrolidinyl amide–anthracene adduct (+)-(11*S*)-**103** using LAH as the reducing reagent. We found that increasing the amount of the reducing reagent led to decrease the percentage yield. The adduct (+)-(11*S*)-**103** was reduce by 5.0 equivalents of LAH at –78 °C to room temperature for 2 days to obtain the highest percentage yield as shown in entry 2. Also, the other optically active form was reduced *via* this condition. The products were purified by flash column chromatography (MeOH/EtOAc/ hexane = 1:4:5 as eluent) as shown in Scheme 28.

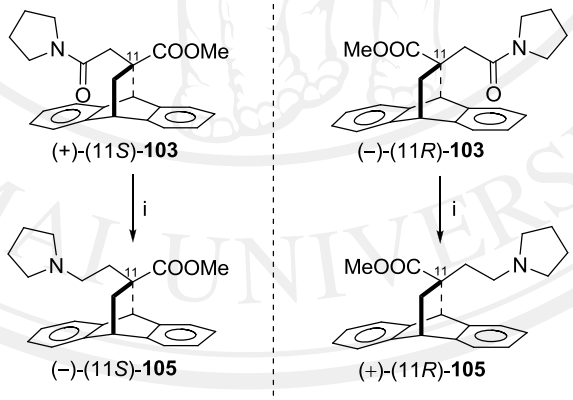

Scheme 28 Synthesis of optically active *N*,*O* heteroatoms TADDOLs–anthracene adducts (+)-(11*S*)-**105** and (–)-(11*R*)-**105**. *Reagents and conditions*: (i) 5.0 equiv LAH, THF, reflux, N_2, 2 days.

The structure of the optically active *N*,*O* heteroatoms TADDOLs–anthracene adducts (+)-(11*S*)-**105** and (–)-(11*R*)-**105** were confirmed by NMR spectral which is shown Figure 19. The signal of proton H_a, H_b, H_c and H_d at 1.09-1.40 ppm as multiplet, proton H_e and H_f at 2.25 ppm as doublet of doublet of doublet (J = 12.8, 6.4

and 2.9 Hz) and 2.84 ppm as doublet of doublet of doublet (J = 12.8, 10.2 and 2.6 Hz), proton H_g and H_h at 2.74 ppm as doublet (J = 11.7 Hz) and 3.11 ppm as doublet (J = 11.7 Hz), proton H_x at 4.19 as triplet (J = 2.4 Hz), H_y at 4.38 ppm as singlet, proton of –OH at 2.88 as broad singlet and aromatic protons at 6.93-7.45 ppm as multiplet. In addition, the protons on pyrrolidine ring, which are four protons on methylene C-2′′′ and methylene C-3′′′ showed signal at 1.68-1.86 ppm as multiplet and four protons methylene C-1′′′ and methylene C-4′′′ at 2.48-2.66 ppm as multiplet.

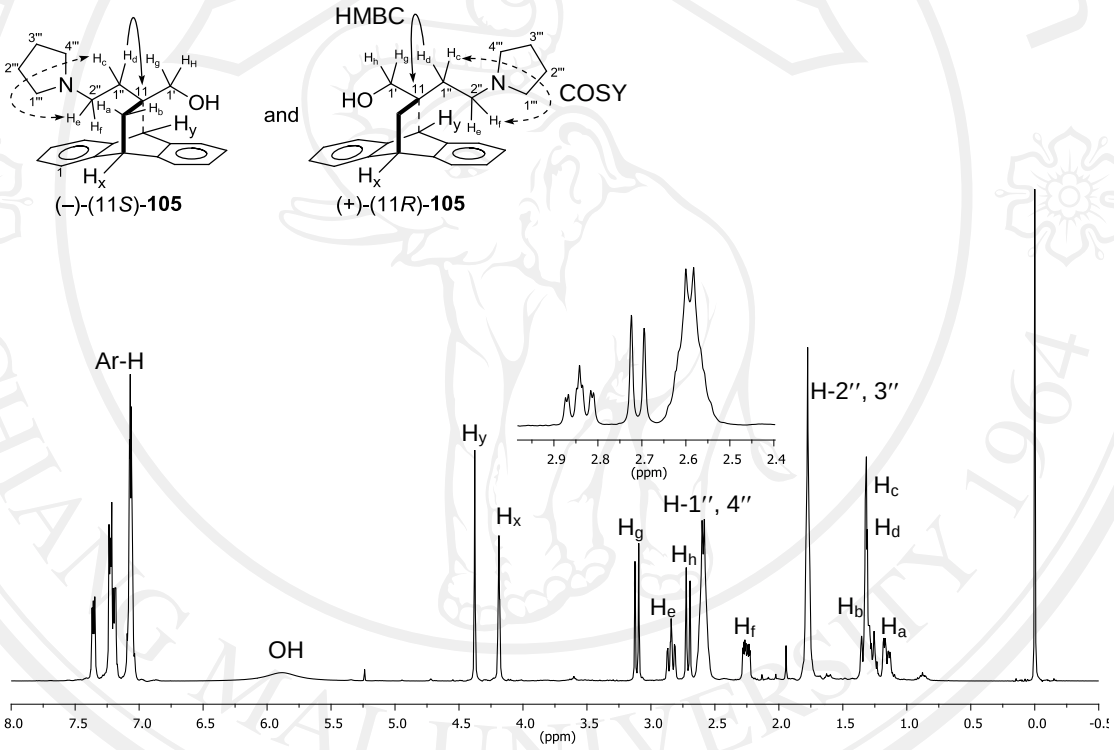

Figure 19 ^{1}H-NMR spectral data of the optically active *N*,*O* heteroatoms TADDOLs–anthracene adducts (+)-(11*S*)-**105** and (–)-(11*R*)-**105** (Dash arrows and plain arrows were COSY and HMBC correlation)

The correlation protons on H_a, H_b, H_c H_d, H_e, H_f, H_g, H_h and protons on pyrrolidine ring were confirmed by COSY correlation. Besides, HMQC correlation showed that H_g and H_h correlated with methylene C-1′, H_c and H_d correlated with methylene C-1′′, H_e and H_f correlated with methylene C-2′′ and protons on pyrrolidine ring correlated with C-1′′′, C-2′′′, C-3′′′ and C-4′′′. HMBC correlation showed that proton H_c and H_d correlated with quaternary C-11, methylene C-1′ and

methylene C-2′′. In contrast, the proton H_e and H_f shows HMBC correlation with methylene C-1′′ but no HMBC correlation with quaternary C-11and methylene C-1′. Hence, the quaternary C-11 connected to methylene C-1′′ and methylene C-2′′, respectively.

3.5.2 Reduction reaction of both enantiomerically pure pyrrolidinyl amide–anthracene adducts (+)-(11*S*)-104 and (–)-(11*S*)-104

In case of synthetic (11*S*)-11-hydroxymethylene-11-(2′′-piperidinyl)-9,10-dihydro-9,10-ethanoanthracene, we studied reduction reaction of piperidinyl amide–anthracene adducts (+)-(11*S*)-**104** and (–)-(11*S*)-**104** by various stoichiometric equivalent of lithium aluminium hydride (LAH). The reduction reactions of adduct (+)-(11*S*)-**104** which was used as model reaction gave the results in Table 28.

Table 28 Optimization of conditions for reduction reaction of piperidinyl amide–anthracene adduct (+)-(11*S*)-**104**

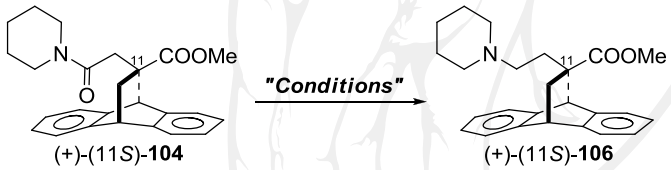

(+)-(11*S*)-**104** (+)-(11*S*)-**106**

Entry	Conditions	Yield (%)[a]	Conversion (%)
1	5.0 equiv LAH, THF, reflux, N_2, overnight	82	100
2	5.0 equiv LAH, THF, –78 °C to rt, N_2, 2 days	54	100
3	10.0 equiv LAH, THF, –78 °C to rt, N_2, 2 days	67	100
4	15.0 equiv LAH, THF, –78 °C to rt, N_2, 2 days	63	100

[a] Isolated yield

As can be seen from Table 28, the reduction reactions of piperidinyl amide–anthracene adduct (+)-(11*S*)-**104** using LAH as the reducing reagent are shown in entry 1-4. They were found that the amount of the reducing reagent increased from 5.0 equivalent to 10.0 equivalent led to increase the percentage yield (entry 2 and 3) but increasing the amount of the reducing reagent from 10.0 equivalent to 15.0 equivalent led to a little bit decrease the percentage yield (entry 3 and 4). However, the adduct (+)-(11*S*)-**104** was reduce by 5.0 equivalents of LAH under reflux for overnight to give the highest percentage yield as shown in entry 1. Consequently, the

other optically active form was reduced *via* this condition. The products were purified by flash column chromatography (MeOH/EtOAc/ hexane = 1:4:5 as eluent) as shown in Scheme 29.

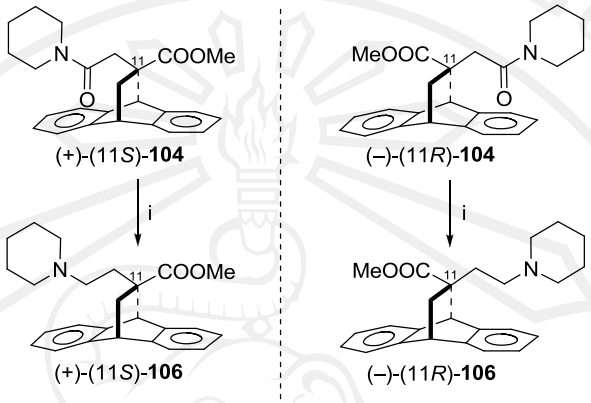

Scheme 29 Synthesis of optically active *N,O* heteroatoms TADDOLs–anthracene adducts (+)-(11*S*)-**106** and (–)-(11*R*)-**106**. *Reagents and conditions*: (i) 5.0 equiv LAH, THF, reflux, N_2, overnight.

In Figure 20 shown NMR spectral of the optically active *N,O* heteroatoms TADDOLs–anthracene adducts (+)-(11*S*)-**106** and (–)-(11*R*)-**106**. The signal of proton H_a, H_b, H_c and H_d at 1.09-1.34 ppm as multiplet, proton H_e and H_f at 2.17 ppm as doublet of doublet of doublet (J = 13.3, 6.88 and 2.7 Hz) and 2.55 ppm as doublet of doublet of doublet (J = 13.3, 9.5 and 2.6 Hz), proton H_g and H_h at 2.72 ppm as doublet (J = 11.8 Hz) and 3.08 ppm as doublet (J = 11.8 Hz), proton H_x at 4.19 as triplet (J = 2.6 Hz), H_y at 4.34 ppm as singlet and aromatic protons at 6.94-7.43 ppm as multiplet. In addition, the protons on piperidine ring, which are two protons on methylene C-3′′′ showed signal at 1.09-1.34 ppm as multiplet, four protons on methylene C-2′′′ and methylene C-4′′′ showed signal at 1.53–1.72 ppm as multiplet and four protons methylene C-1′′′ and methylene C-5′′′ at 2.22–2.67 ppm as multiplet. The correlation protons on H_a, H_b, H_c H_d, H_e, H_f, H_g, H_h and protons on pyrrolidine ring were confirmed by COSY correlation. Besides, HMQC correlation showed that H_g and H_h correlated with methylene C-1′, H_c and H_d correlated with methylene C-1′′, H_e and H_f correlated with methylene C-2′′ and protons on pyrrolidine ring correlated with C-1′′′, C-2′′′, C-3′′′, C-4′′′ and C-5′′′. HMBC correlation showed that proton H_c and H_d correlated with quaternary C-11, methylene C-1′ and methylene C-2′′. In

contrast, the proton H_e and H_f shows HMBC correlation with methylene C-1′′ but no HMBC correlation with quaternary C-11and methylene C-1′. Hence, the quaternary C-11 connects to methylene C-1′′ and methylene C-2′′, respectively.

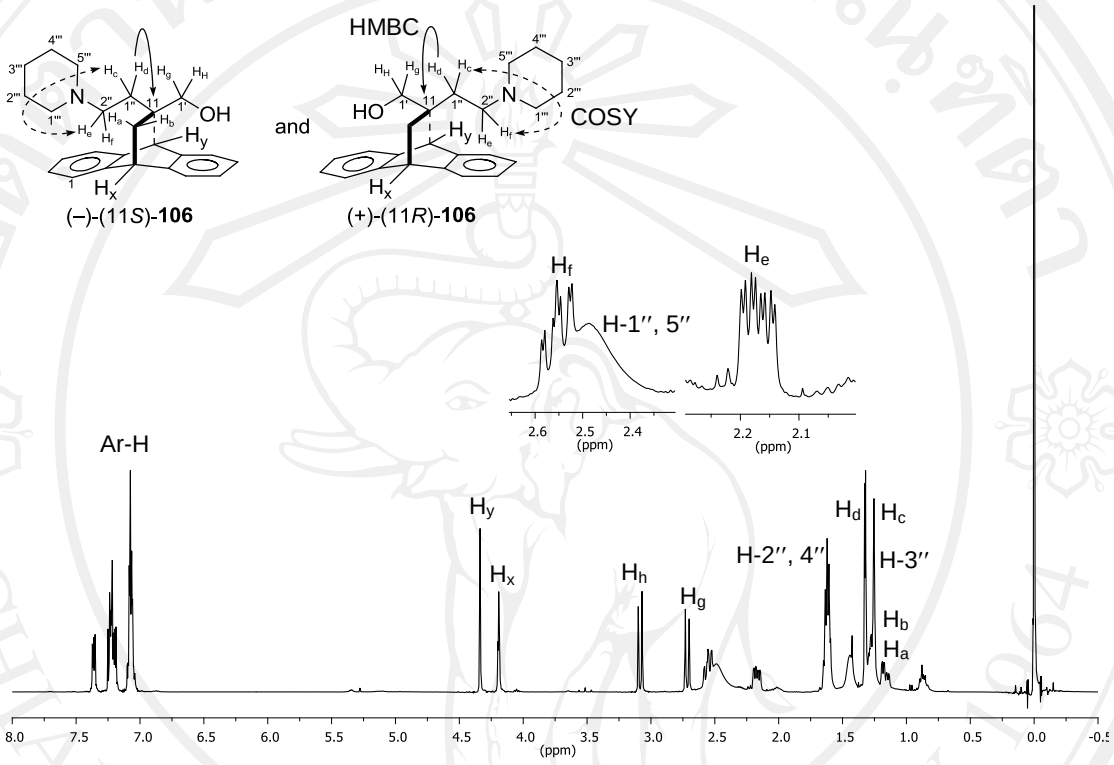

Figure 20 ^{1}H-NMR spectral data of the optically active *N*,*O* heteroatoms TADDOLs–anthracene adducts (+)-(11*S*)-**106** and (–)-(11*R*)-**106** (Dash arrows and plain arrows were COSY and HMBC correlation)

3.5.3 Reduction reaction of optically active pure (pyrrolidinyl or piperidinyl) spiro–lactone anthracene adducts (+)-(4′*S*,11*R*)-107a and (+)-(4′*S*,11*R*)-108a

In this study, we focused on synthesis of *N*,*O* heteroatoms TADDOLs–anthracene adducts (+)-(4′*S*,11*R*)-**109** and (+)-(4′*S*,11*R*)-**110** by reducing the amide spiro–lactone anthracene adducts (+)-(4′*S*,11*R*)-**107a** and (+)-(4′*S*,11*R*)-**108a**, respectively. The results of these reactions are summarized in Table 29.

Table 29 Optimization of conditions for reduction reaction of amide spiro–lactone anthracene adducts (+)-(4′*S*,11*R*)-**107a** and (+)-(4′*S*,11*R*)-**108a**

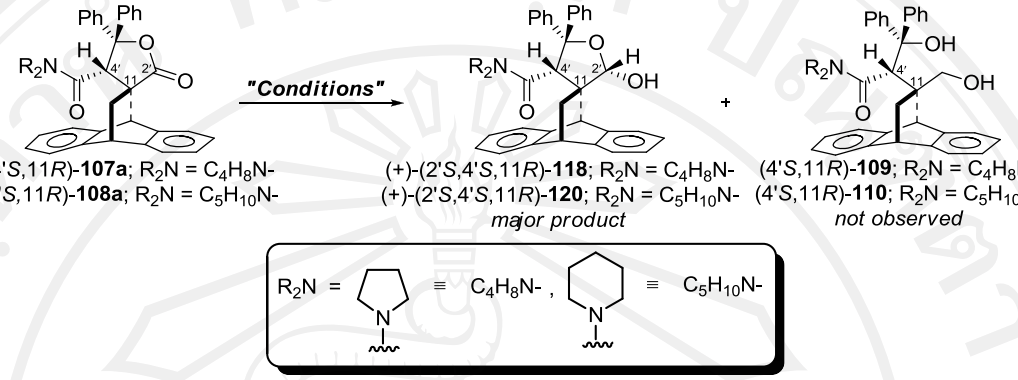

Entry	R_2N	Conditions	Yield (%)[a]	Conversion (%)
1	C_4H_8N-	7.0 equiv LAH, THF, –78 °C to rt, N_2, 3 h	83	100
2		7.0 equiv LAH, THF, –78 °C to rt, N_2, 6 h	90	100
3		7.0 equiv LAH, THF, –78 °C to rt, N_2, 24 h	71	100
4		7.0 equiv LAH, THF, –78 °C to rt, N_2, 3 days	64	100
5		20.0 equiv LAH, THF, –78 °C to rt, N_2, 24 h	76	100
6		20.0 equiv LAH, THF, –78 °C to rt, N_2, 3 days	83	100
8	$C_5H_{10}N$-	7.0 equiv LAH, THF, –78 °C to rt, N_2, 3 days	78	100
9		20.0 equiv LAH, THF, –78 °C to rt, N_2, 3 days	55	100

[a] Isolated yield

Form the results in Table 29, the target products which are *N*,*O* heteroatoms TADDOLs–anthracene adducts (+)-(4′*S*,11*R*)-**109** and (+)-(4′*S*,11*R*)-**110** did not obtain in the reduction reactions of amide spiro–lactone anthracene adducts by using LAH as reducing reagent. However, these reduction reactions gave adducts **118** and **120** as major product. The reduction reactions of adducts **107a** and **108a** with LAH could be explained in Scheme 30. Hydride of LAH attacked at carbonyl group of spiro–lactone ring follow by ring opening to give transition state **A**. After that, transition state **A** cyclized via 5-exo-trig cyclization to provide adduct **118** and **120** which instead of hydride nucleophilic addition at carbonyl group of aldehyde to obtain the target product **109** and **110**.

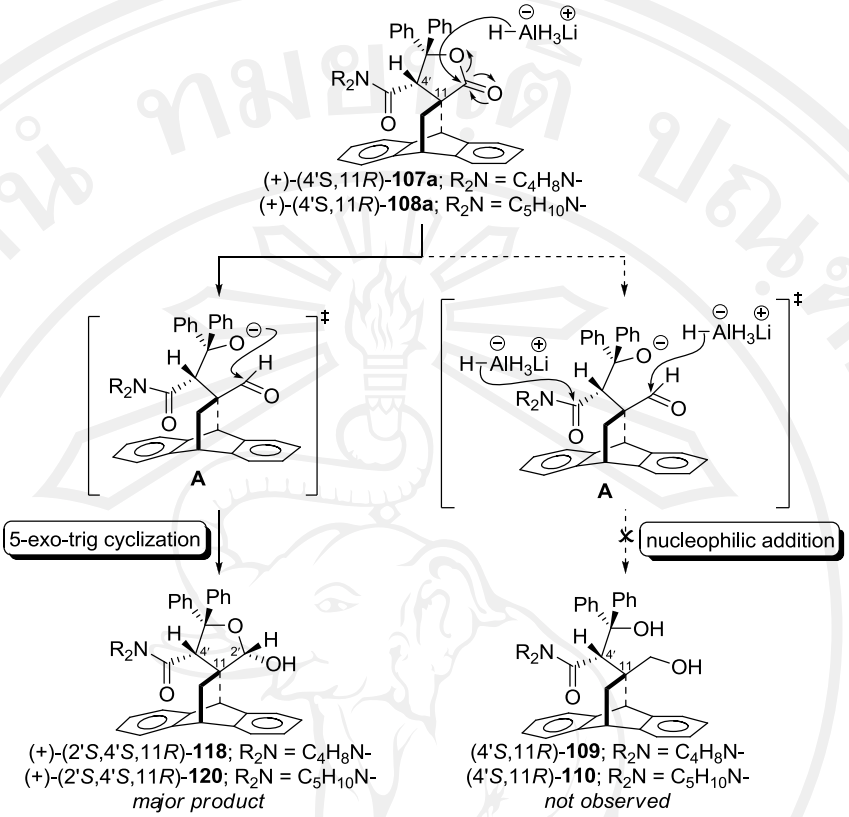

Scheme 30 Proposed mechanism of cyclization reaction and nucleophilic addition reaction for the reduction reaction of amide spiro–lactone anthracene adducts (+)-(4′*S*,11*R*)-**107a** and (+)-(4′*S*,11*R*)-**108a**.

The structure of adduct (+)-(2′*S*,4′*S*,11*R*)-**118** can be confirmed by NMR and NOE experiment. The ^{1}H-NMR spectrum of this adduct is illustrated in Figure 21. The signal of proton H_a, H_b and H_x appeared at 1.32, 1.47 and 4.11 ppm (*ABX* system, (J = 13.2, 2.9 and 2.6 Hz), proton H_c at 3.32 ppm as singlet, proton H_d at 4.49 as doublet (J = 12.4 Hz), proton H_y at 4.71 ppm as singlet, aromatic protons at 6.61-7.62 ppm as multiplet and proton of –OH at 8.22 as doublet (J = 12.4 Hz). In addition, the signal of protons on pyrrolidine ring, which are one proton on methylene C-9′ appeared at 1.55-1.73 ppm as multiplet, two protons methylene C-8′ appeared at 1.77-1.96 ppm as multiplet and one proton on methylene C-10′ appeared at 2.41-2.54 ppm as multiplet, one proton on methylene C-7′ appeared at 2.79-2.89 ppm as multiplet and the other protons of methylene C-7′ and C-10′ appeared at 3.28-3.44 ppm as multiplet. The correlation protons on H_a, H_b, H_c and protons on pyrrolidine ring were confirmed by COSY correlation. Besides, HMQC correlation showed that

H_c correlated with methylene C-4′, H_d correlated with C-2′ and protons on pyrrolidine ring correlated with C-7′, C-8′, C-9′ and C-10′. HMBC correlation showed that proton H_c correlated with quaternary C-6′ and H_d correlated with C-11.

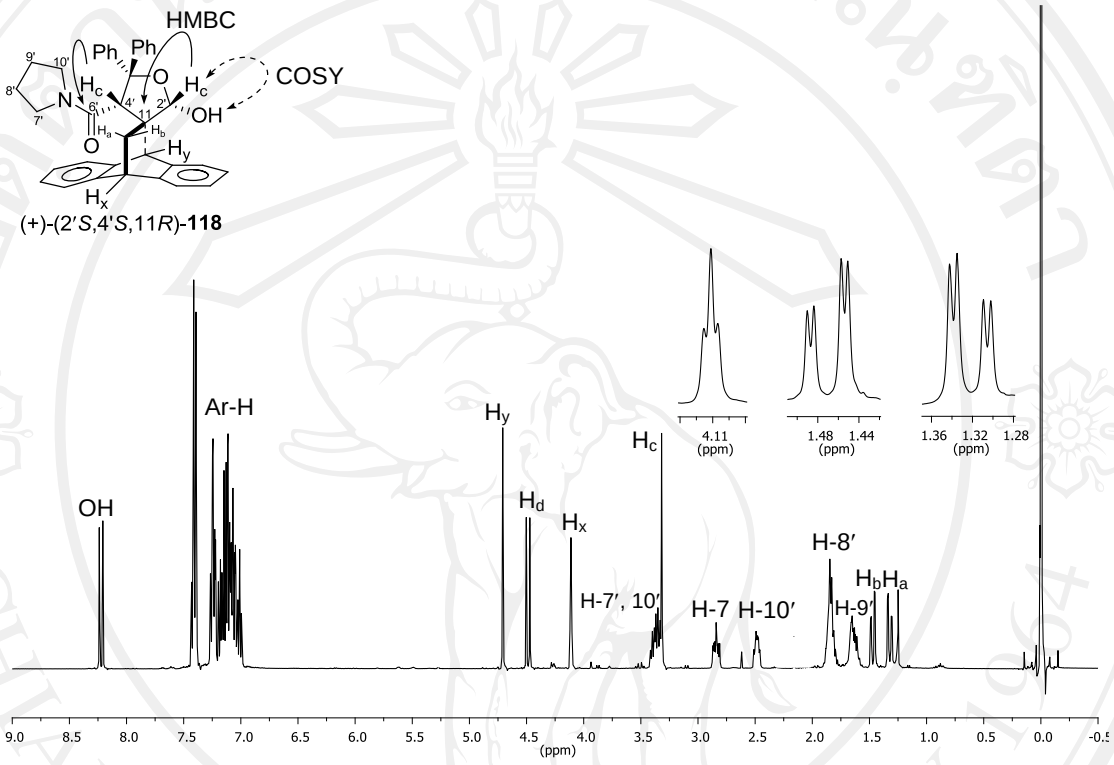

Figure 21 ^{1}H-NMR spectral data of adduct (+)-(2′*S*,4′*S*,11*R*)-**118** (Dash arrows and plain arrows were COSY and HMBC correlation)

From NOE experiment, it illustrated that the irradiation of the proton H_c gave NOE effect with the proton H_a but no NOE effect with the proton H_y. Hence, the orientation of the proton H_c is on the upper face and *syn*- with the proton H_a but *anti*- with the proton H_y. In addition, the proton H_d enhanced with the proton H_b but no NOE effect with the proton H_y. Also, the orientation of the proton H_d is on the upper face and *syn*- with the proton H_b but *anti*- with the proton H_y. Besides, the structure of adduct (+)-(2′*S*,4′*S*,11*R*)-**118** could be confirmed by MM2 force field calculations for energy minimization from modeling program ChemBio3D Ultra 11.0 program as depicted in Figure 22. Result of adduct (+)-(2′*S*,4′*S*,11*R*)-**118** showed that the distance form H_c to H_a, H_c to H_y, H_d to H_b and H_d to H_y are 2.10, 3.70, 2.10 and 3.88

Å, respectively. The results from computational calculation are in agreement with the NOE results.

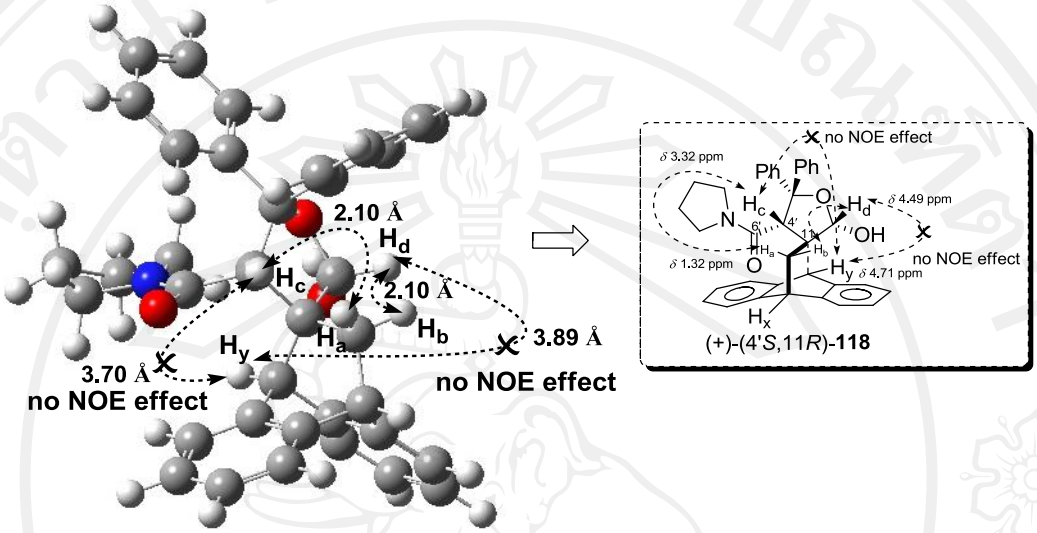

Figure 22 3D structure conformation of adduct (+)-(2′*S*,4′*S*,11*R*)-**118** was generated by MM2 force field calculations for energy minimization from modeling program Chem3D Ultra 11.0 and GaussView 3.09 program with the observed NOE correlations (arrows)

Additionally, The structure of adduct (+)-(2′*S*,4′*S*,11*R*)-**120** was confirmed by NMR technique. The ^{1}H-NMR spectrum of this adduct is depicted in Figure 23. The signal of proton H_a, H_b and H_x appeared at 1.31, 1.49 and 4.10 ppm (*ABX* system, (J = 13.2, 2.8 and 2.9 Hz), proton H_c at 3.59 ppm as singlet, proton of H_d at 4.46 as doublet (J = 12.4 Hz) proton H_y at 4.67 ppm as singlet, aromatic protons at 6.96–7.50 ppm as multiplet and proton of –OH at 8.33 as doublet (J = 12.4 Hz). Furthermore, the signal of protons on piperidine ring, which are one proton on methylene C-8′ appeared at 1.08-1.24 ppm as multiplet, five protons on methylene C-8′, methylene C-9′ and methylene C-10′ appeared at 1.43–1.66 ppm as multiplet, two protons methylene C-11′ appeared at 2.83–2.99 and 3.11–3.21 ppm as multiplet and two proton of methylene C-7′ appeared at 3.11–3.21 and 3.30–3.46 ppm as multiplet. The correlation protons on H_a, H_b, H_c and protons on piperidine ring were confirmed by COSY correlation. Moreover, HMQC correlation showed that H_c correlated with methylene C-4′′, H_d correlated with C-2′ and protons on piperidine ring correlated

with C-7′, C-8′, C-9′, C-10′ and C-11′. HMBC correlation showed that proton H_c correlated with quaternary C-6′ and H_d correlated with C-11.

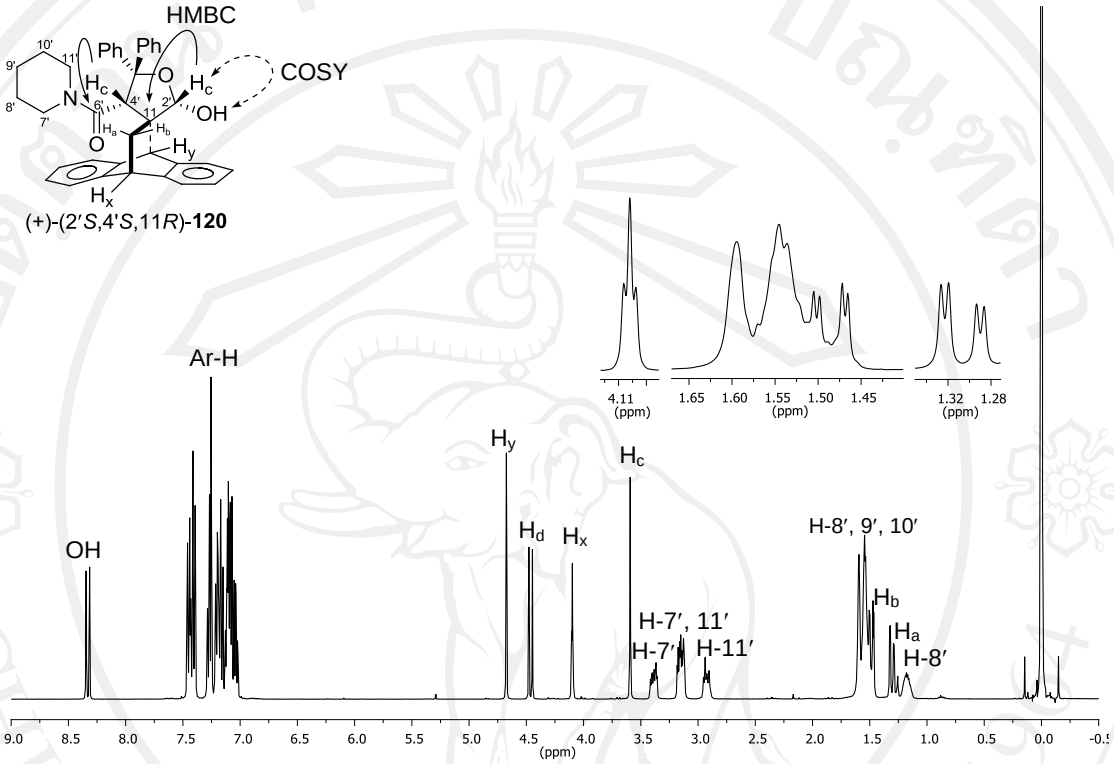

Figure 23 ^{1}H-NMR spectral data of adduct (+)-(2′*S*,4′*S*,11*R*)-**120** (Dash arrows and plain arrows were COSY and HMBC correlation)

The stereochemistry of adduct (+)-(2′*S*,4′*S*,11*R*)-**120** can be confirmed by NOE technique, it illustrated that the irradiation of the proton H_c gave NOE effect with the proton H_a but no NOE effect with the proton H_y. Hence, the orientation of the proton H_c is on the upper face and *syn*- with the proton H_a but *anti*- with the proton H_y. In addition, the proton H_d enhanced with the proton H_b but no NOE effect with the proton H_y. Also, the orientation of the proton H_d is on the upper face and *syn*- with the proton H_b but *anti*- with the proton H_y. Besides, the structure of adduct (+)-(2′*S*,4′*S*,11*R*)-**120** could be confirmed by MM2 force field calculations for energy minimization from modeling program ChemBio3D Ultra 11.0 program as depicted in Figure 24. Result of adduct (+)-(2′*S*,4′*S*,11*R*)-**120** showed that the distance form H_c to H_a, H_c to H_y, H_d to H_b and H_d to H_y are 2.05, 3.66, 2.15 and 3.74 Å, respectively. The results from computational calculation are in agreement with the NOE results.

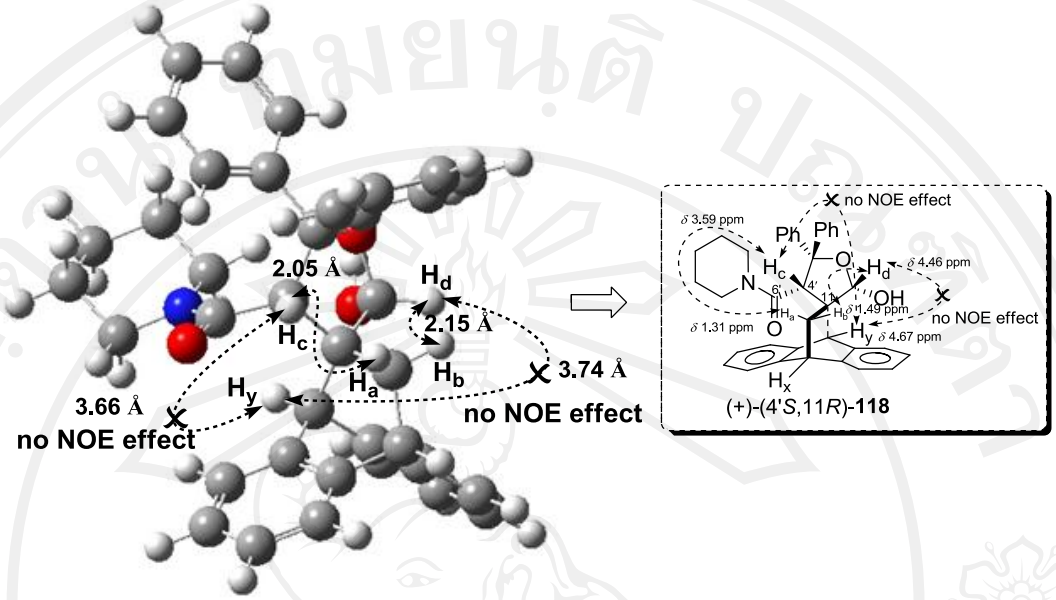

Figure 24 3D structure conformation of adduct (+)-(2′*S*,4′*S*,11*R*)-**120** was generated by MM2 force field calculations for energy minimization from modeling program Chem3D Ultra 11.0 and GaussView 3.09 program with the observed NOE correlations (arrows)

In case of reduction reaction of pyrrolidinyl amide spiro–lactone anthracene adduct and piperidinyl amide spiro–lactone anthracene adduct in Table 29 (entry 1 and 8) gave adduct **122** as by-product which was explained in Scheme 31. ^{1}H-NMR spectral of by-product **122** was found that the signal of proton H_d and H_c appeared at 2.15 and 2.38 ppm as doublet (J = 17.4 z), proton H_e and H_f shown the signal at 3.70 and 4.00 ppm as doublet (J = 9.3 Hz). HMBC correlation indicated the connectivity between H_c, H_d, H_e and H_f with quaternary C-5′. Moreover, the correlation between H_c and H_d, H_e and H_f were confirmed by COSY correlation (Figure 25).

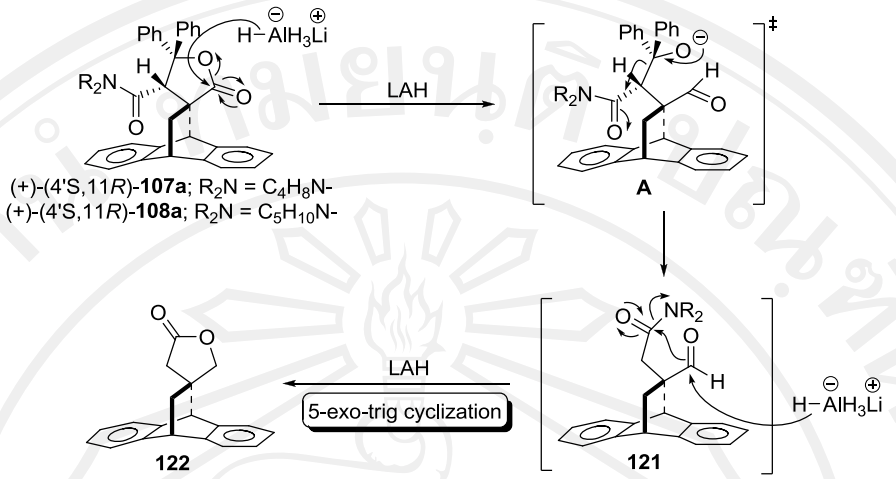

Scheme 31 Proposed mechanism of cyclization reaction gave by-product **122**.

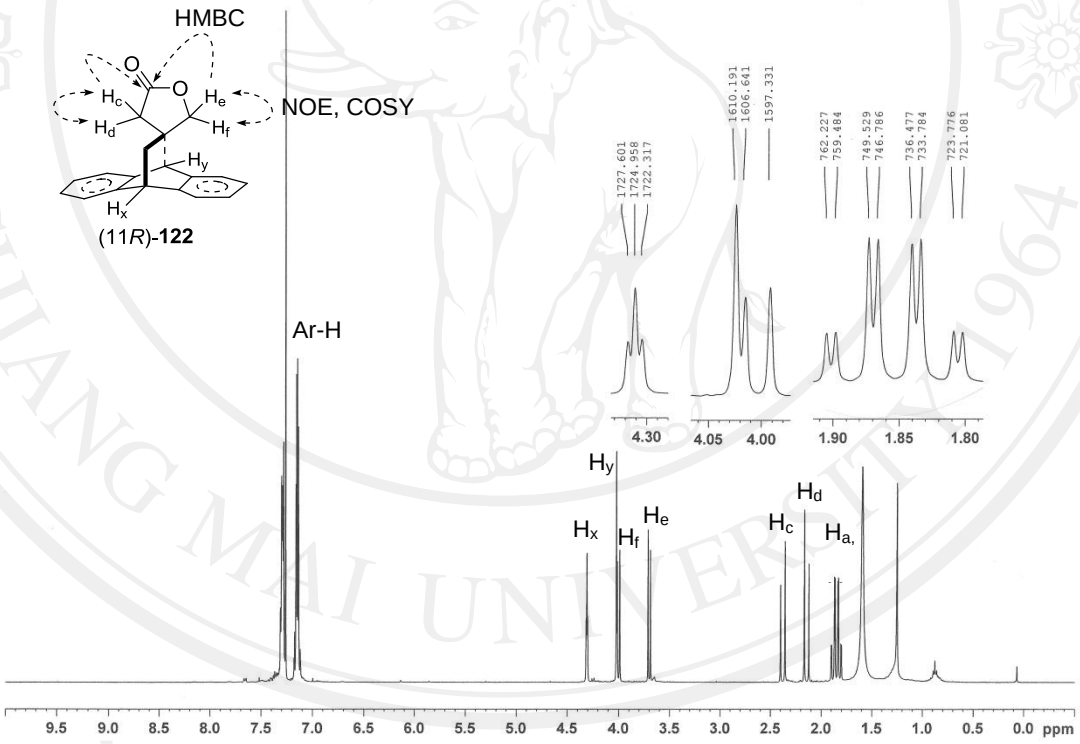

Figure 25 ^{1}H-NMR spectral data of by-products (11*R*)-**79** and (11*S*)-**79** (Dash arrows and plain arrows were COSY, NOE and HMBC correlation, respectively)

From unsuccessful of synthetic *N*,*O* heteroatoms TADDOLs–anthracene adducts (+)-(4′*S*,11*R*)-**109** and (+)-(4′*S*,11*R*)-**110** in the previous conditions, we interested in synthesis of these adducts by the hard condition which is refluxing for overnight. The results are summarized in Scheme 32. The products which were

obtained in reduction reaction of amide spiro–lactone anthracene adduct by refluxing with LAH can be explained in the Scheme 33.

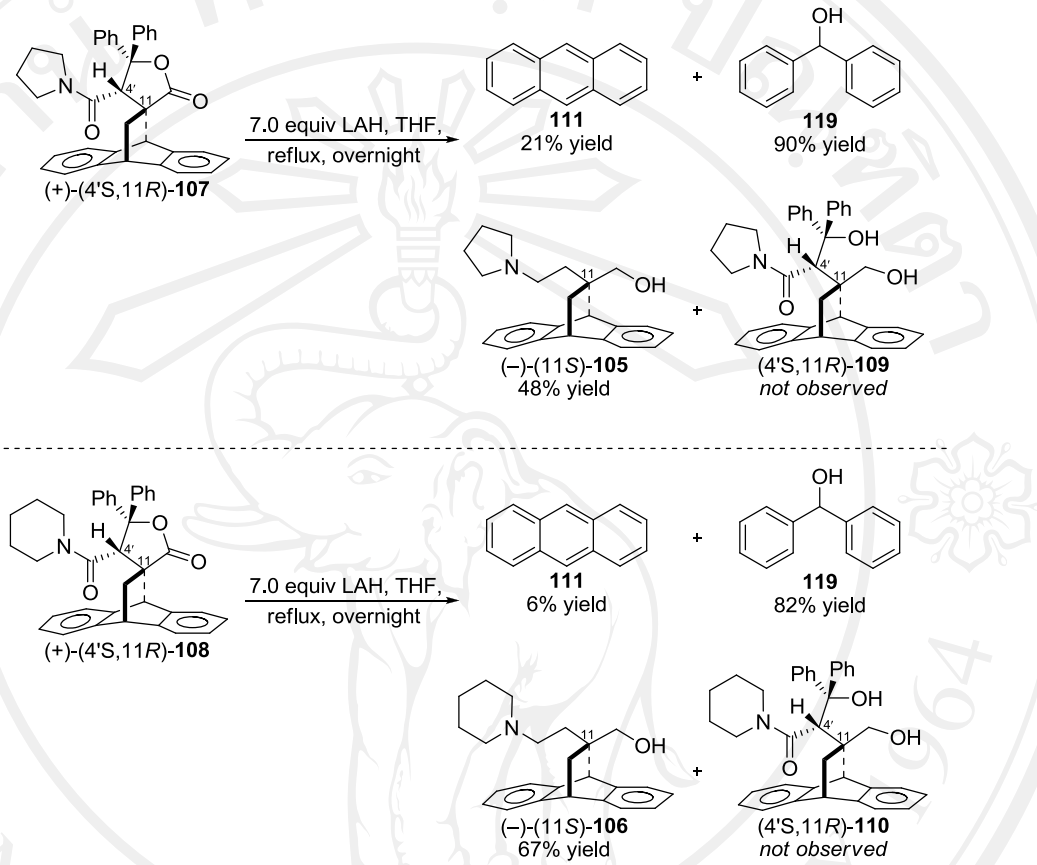

Scheme 32 Reduction reaction of amide spiro–lactone anthracene adducts (+)-(4′*S*,11*R*)-**107** and (+)-(4′*S*,11*R*)-**108** by refluxing for overnight.

Form studying reduction reactions of amide spiro–lactone anthracene adducts were found that the *N*,*O* heteroatoms TADDOLs–like anthracene adducts (+)-(4′*S*,11*R*)-**109** and (+)-(4′*S*,11*R*)-**110** were not observed in these condition. Also, these adducts may be not synthesized *via* reduction reaction by using lithium aluminium hydride (LAH).

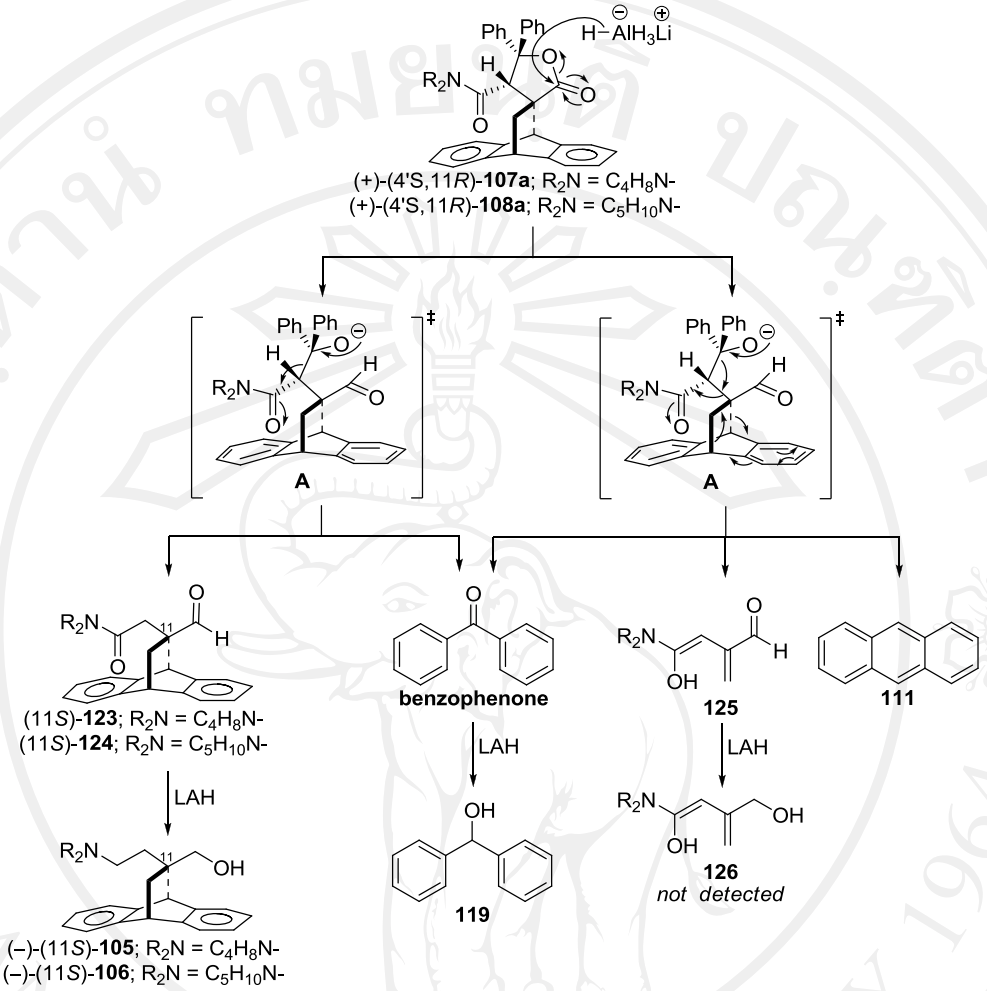

Scheme 33 Proposed mechanism of reduction reaction amide spiro–lactone anthracene adducts (+)-(4′*S*,11*R*)-**107a** and (+)-(4′*S*,11*R*)-**108a** by refluxing with LAH.